



Evaluation of groundwater quality and human health risks from fluoride and nitrate in semi-arid region of northern India

Gagandeep Singh · Madhuri S. Rishi · Rajkumar Herojeet · Lakhvinder Kaur · Kirti Sharma

Received: 22 February 2019 / Accepted: 3 October 2019 / Published online: 5 November 2019
© Springer Nature B.V. 2019

Abstract Groundwater quality in the alluvial plains of Punjab has special significance and needs great attention since it is the foremost source of drinking, irrigation and industrial uses. The present research work emphasizes the integrated hydrogeochemical and chemometric statistical approaches to appraise the geochemical processes and source apportionment of the groundwater in the alluvial plains of Jalandhar district, Punjab, India. The human health risk assessment was also performed to quantify the potential non-carcinogenic impacts of nitrate and fluoride on human health through ingestion of groundwater. For this purpose, 41 groundwater samples were collected from different groundwater abstraction units and analysed for pH, electrical conductivity, total dissolved solids, total hardness, total alkalinity and major ions (Ca^{2+} ,

Mg^{2+} , Na^+ , K^+ , HCO_3^- , CO_3^{2-} , SO_4^{2-} , NO_3^- , F^- , Cl^- and PO_4^{3-}) using standard protocols. Drinking water quality index and Revelle index showed that groundwater samples fall under poor to unfit water class and salinization along the south-western portion of the study region shows poor water quality. The results of the hazard index ($\text{HI}_{\text{ingestion}}$) show 68% and 46.34% of the groundwater samples have $\text{HI} > 1$ for children and adults. The non-carcinogenic health risk assessment of nitrate (NO_3^-) and fluoride (F^-) on the local population indicated that the children are more vulnerable through direct ingestion of drinking water than adults. Piper diagram and saturation index reveal that $\text{Ca}^{2+}\text{-Mg}^{2+}\text{-HCO}_3^-$ is the dominant hydrochemical facies and oversaturated with calcite, dolomite and aragonite minerals in the groundwater. Gibbs diagrams, chloro-alkaline indices and scatter plots show that the hydrochemistry of the groundwater is mainly governed by aquifer material interaction such as weathering of silicate, carbonate rock, halite dissolution and cation exchange process. Chemometric statistical techniques revealed that the source identification of parameters such as Ca^{2+} , Mg^{2+} , Na^+ , K^+ , HCO_3^- , CO_3^{2-} and F^- is originated from geogenic factors, whereas NO_3^- , SO_4^{2-} , Cl^- and PO_4^{3-} are from the anthropogenic origin. Therefore, urgent and efficient measures must be taken to combat groundwater pollution and reduce human health risk in the study area.

Electronic supplementary material The online version of this article (<https://doi.org/10.1007/s10653-019-00449-6>) contains supplementary material, which is available to authorized users.

G. Singh · M. S. Rishi (✉) · L. Kaur
Department of Environment Studies, Panjab University,
Chandigarh, India
e-mail: madhuririshi@gmail.com

R. Herojeet
Department of Environment Studies, Post Graduate
Government College-11, Chandigarh, India

K. Sharma
University Institute of Engineering and Technology,
Panjab University, Chandigarh, India

Keywords Alluvial plains · Chemometric statistical techniques · Groundwater quality · Hazard index · Hydrogeochemical

Introduction

Groundwater is considered a substantial source for drinking, agricultural and industrial activities in the semi-arid parts of India. Urban, semi-urban and rural areas of Indian states are mainly reliant on groundwater as approximately 85% rural domestic water demands and 50% urban potable water requirements are fulfilled by groundwater only (Ahada and Suthar 2018a; Jain and Vaid 2018). India is the first largest user of groundwater in the world with 251 km³/year abstraction rate followed by China (112 km³/year) and USA (112 km³/year). Out of the total amount of groundwater extracted, largest share ~ 89% is used by the agricultural sector particularly for irrigation purpose and remaining 11% for public water (domestic purpose) and industrial supply (World bank 2012; Margat and Gun 2013; Raju and Singh 2017; Singh et al. 2019b; Ahada and Suthar 2018b). Groundwater plays a crucial role in the socio-economic, agricultural and environmental development of a region (Kaur and Rishi 2018). Anthropogenic activities like unplanned industrialization, unsustainable economic development, rapid population growth and overexploitation of groundwater in the past few decades had posed a severe threat on this precious resource in terms of both quantity and quality (Sharma et al. 2017; Pant et al. 2017b; Kaur et al. 2019). During the green revolution, farmers of Punjab have extensively followed the monocropping culture (mainly wheat–rice cycle), instead of multiple cropping by abandoning other crops like pulses, mustard and vegetables due to fertile alluvial plain and their surplus availability of water resource. Intensive use of fertilizers and pesticides act as diffuse pollutants originating from irrigated agricultural field, so the fertilizers and pesticides are the main responsible factors affecting the quality of the aquifers. Thus, nutrients in the form of NO₃⁻, PO₄³⁻ and K⁺ are common contaminants in soils and groundwater. The chemical contamination of groundwater from both natural and anthropogenic factors is almost an irreversible process (Causapé et al. 2006; Aydi 2018). Further, the long-term consumption of

contaminated water is of great concern due to possible health risks. Besides heavy metals, nitrate and fluoride are known to be harmful to children and adults because of their low tolerance towards the pollutants. The human exposure to these metals is mainly through ingestion and dermal contacts. The non-carcinogenic human health risks from NO₃⁻ and F⁻ in groundwater have been enlisted as an emerging issue in our country. The health hazard associated with the consumption of NO₃⁻-rich water is methemoglobinemia in newly born children, and thyroid dysfunctions and hypertension in adults and pregnant women (Ahada and Suthar 2018b). Furthermore, ~ 200 million people around the globe are regularly consuming water contaminated with F⁻ content above the limits of WHO 2011 (Emenike et al. 2018). Also, the ingestion of high-F⁻-content water may cause dental fluorosis, osteoporosis, arthritis and thyroid. Therefore, the toxicity effects of NO₃⁻ and F⁻ are needed to assess their non-carcinogenic health risks on human health expose at any dose.

Jalandhar is a predominantly agricultural district in the central part of Punjab (commonly known as the Bist Doab tract) with cropping intensity of 178%. Around 90% of the total irrigated area is fulfilled by groundwater. The region also witnessed a considerable increase in the density of the tube wells, i.e. 38% from 1998 to 2013 (Dhillon et al. 2019). The high annual rate of groundwater extraction (8600 m³/ha/a), chiefly for agricultural purposes, has turned most of the blocks into the ‘overexploited’ category in the region (Rao et al. 2017). The district witnessed expansion of agricultural land by illegally converting forest area to increase paddy cultivation area has led to tremendous stress on groundwater. The area received very low seasonal rainfall (70.3 cm/year), which is unable to support the high-water demanding agricultural crops. Thus, groundwater mining is the only available option to sustain the agricultural productivity in the fertile alluvial plains of the Indo-Gangetic region. Farmers are extensively using agrochemical fertilizers on highest scale of consumption rate, i.e. 251 kg/ha as compared to the national average of 165.8 kg/ha to maintain the productivity (World Bank; Government of Punjab 2016). As per the recent report of the Punjab Department of Agriculture, the demand of N, P and K fertilizers in the study area has increased significantly from 37.50 kg/ha/year in 1970 to 257 kg/ha/year in 2016. The conversion of

conventional farming practices (organic method) to synthetic agrochemical techniques has largely disturbed the various segments of environmental dynamics and affects the non-target species due to release of toxic persistent chemicals. The water-soluble chemicals are dissolved in irrigated water and percolated into subsurface strata, thus affecting the natural chemical equilibrium of aquifer system (Singh et al. 2015; Pant et al. 2017, 2019). Thus, the prolonged consumption of chemical-contaminated groundwater is one of the threatening factors for human health risk, cattle and beneficial soil microbes. Jalandhar district has nearly 21 large- and medium-scale and 20,295 small-scale industries and is also famous for manufacturing various sports good in the country (Government of Punjab 2016). Industrial clusters such as tanneries, paper and textile industries are mainly located in the vicinity of the Jalandhar city. Industrial and urban sectors not only utilize the available water, but also generate a large amount of wastewater of complex nature (Aulakh et al. 2009). Moreover, the study area lacks proper sewerage or drainage system where wastewater is directly discharged into nearby streams and river. It results in the increasing vertical and lateral spread of pollutants in aquifer system, rendering serious threats to environmental health (Mukate et al. 2018).

Some researchers have already carried out studies focusing on the basic quality appraisal of groundwater for drinking and irrigation purposes in this region (Purushothaman et al. 2012, 2014; Singh et al. 2019a; Rao et al. 2015). Research on groundwater contamination and associated human health risks is rather limited. To fulfil the loopholes of the previous study, the integrated approach of multivariate statistical techniques along with GIS, hydrogeochemical modelling and human health risk assessment was employed as robust methods to understand the geochemical signatures and water quality appraisal in the alluvial aquifer of north-east Punjab (Herojeet et al. 2015, 2016; Li et al. 2016, 2018a; Rao et al. 2017; Singh et al. 2019b; Keesari et al. 2019; Kaur et al. 2019). The emergence of hydrogeochemical characterization techniques and chemometric modelling enables to overcome the limitation of conventional study of using various water quality indices and graphical representation to define pollution source of groundwater in Jalandhar district. Chemometric techniques such as principal component analysis (PCA)

and cluster analysis (CA) along with geographical information system (GIS) techniques aid in the interpretation of the large dataset for a better understanding of the geochemical evolution and sources of the pollution in the alluvial aquifers (Singh et al. 2019b; Herojeet et al. 2017; Rajkumar et al. 2018). The major objectives of the present research were to assess the quality appraisal of groundwater for drinking and agricultural purposes, to understand hydrogeochemical evolution through graphical modelling, to elucidate the source apportionment related to anthropogenic and natural sources with the help of chemometric and GIS techniques and to assess the non-carcinogenic human health risk associated with direct ingestion of groundwater in the agricultural dominated region of the study area. This study will help to maintain the ecological balance with the water resource management in such semi-arid agrarian state of India.

Study area and groundwater scenario

Jalandhar is an agriculturally prosperous district of Punjab situated in the central part of the state and located between 30°59' to 31°37'N latitudes and 75°04' to 75°57'E longitudes (Fig. 1). The district is divided into five taluks, namely Jalandhar I and II, Nakodar, Shahkot and Phillaur. Three distinct seasons are experienced, viz. winter, summer and monsoon. The study area represents semi-arid conditions marked by hot summer and mild winter. The area received an average annual rainfall of 703 mm where 70% of the annual normal rainfall is received during the southwest monsoon from July to September (CGWB 2016, 2018). Temperature in the district varies between a minimum of 5 °C (in January) and a maximum of 45 °C (in May–June). Agriculture sector share is the main economic domestic product and dominant land-use–land-cover (LULC) class in the district (Fig. 2). Wheat and rice are the principal crops grown in the region during Rabi and Kharif seasons, respectively. Jalandhar district is a part of Satluj sub-basin of Indus Basin representing vast Indo-Gangetic alluvial plains and is drained by perennial River Satluj and its tributary *East Bein*. The study area is part of Bist Doab (the area bounded between the River Satluj and Beas) tract comprised of Quaternary to Sub-Recent alluvium type consisting of pebbles,

Table 1 Unit weight of water quality parameters for DWQI

Parameters	Unit weight (W _n)
pH	0.1420
TDS	0.0006
TH	0.0020
Ca ²⁺	0.0060
Mg ²⁺	0.0121
HCO ₃ ⁻	0.0020
NO ₃ ⁻	0.0268
F ⁻	0.8043
Cl ⁻	0.0012
SO ₄ ²⁻	0.0030
∑ W _n	1.0000

gravel, fine- to medium-grained sand, clay and kanker. Two types of alluvium, namely older alluvium (Bhangar) and newer alluvium (Khadar), are available in the region. The older alluvium of Middle to Late Pleistocene age comprises of fine to medium sandy soil, silty clay, loam, sandy loam and sandy clay which is rich in calcareous material occurring all over the district (Supplementary Fig. 3 and Supplementary Table 1). The newer alluvium belongs to Upper Pleistocene to Recent age consists of coarse- to medium-grained sand with a lesser amount of silt and clay and poor in the calcareous matter (Rao et al. 2017; CGWB 2012, 2014). Kanker beds are generally more in older alluvium. Sand sheets of aeolian origin of Recent age from Rajasthan also exist in the western parts of the district (CGWB 2018). Physiographically, the district is prominent by two different features, namely vast alluvial plains and Satluj floodplain (G et al. 2015). Groundwater exists under both unconfined and confined conditions in these alluvial aquifers. Multiple aquifer groups consisting of fine- to coarse-grained sand are present in the study area to the depth of 350 metres below ground level (m bgl). The first aquifer group (up to 115 m bgl) is under unconfined conditions, while the second and the third aquifer groups under semi-confined to confined conditions exist up to 130 to 195 m bgl and 215–333 m bgl, respectively (CGWB 2012, 2016). An average 81 m coarse sand bed which is gravel in nature comprises the aquifer group I, and extensive 24-m-thick clay layer separates the aquifer I from underlying aquifer group II (Rao et al. 2017). Aquifer

group II consists of alternating sequences of thin layers of sand and clay beds and gravel and occasional kankars are also present in this aquifer group. Topographically, it is more or less a flat terrain, having a gentle slope from NE to SW. Long-term water level trend analysis by Central Ground Water Board (CGWB) indicates general decline (negative) up to 8.18 m in the district. The water table elevation varies from 186 to 240 m above mean sea level (a msl) in the study area (Fig. 3). Annual water level analysis indicates that groundwater level decline at the rate of 0.0290 to 1.1398 metres per year. The groundwater flow in the district is towards south-west direction (Fig. 3). All the ten blocks of the district are categorized as ‘overexploited’ with 229% of groundwater development stage (CGWB 2016, 2018). The unconfined aquifer in the study area is under tremendous stress due to the high withdrawal of groundwater for agricultural and domestic purposes.

Materials and methods

Sample collection and analytical procedures

A well-tested systematic random sampling technique was adopted to collect the groundwater samples from the study area. Forty-one samples were collected using Global Positioning System (GPS) during the post-monsoon season (October 2017) from tube wells (TW) and hand pump (HP) in the area under investigation. The geographical locations of all sampling stations are presented in Fig. 1. The standard methods of the American Public Health Association (APHA 2005) were followed for sample collection, transportation, conservation and analytical procedures (Table 2). All the groundwater samples were collected in 1-L high-density polyethylene (HDPE) bottles pre-washed with 10% nitric acid (HNO₃) and rinsed with double-deionized water. Before sampling, the water stored in the well pipes was pumped out for 10–15 min to ensure the original composition of water. All HDPE bottles were thoroughly rinsed three times with the water to be sampled to avoid unpredictable changes in characteristics as per standard protocols. Physical parameters like pH, electrical conductivity (EC) and total dissolved solids (TDS) were measured on site with a portable multiparameter water quality meter (Hanna HI98194). Two sets of groundwater samples

Table 2 Statistical summary of physicochemical parameters of groundwater of the study area

Parameter	Mean ± SD	Range	BIS (2012)		% of sample above BIS (2012)		WHO (2011) Standards		% of sample above WHO (2011) Standards	Undesirable effect produced beyond MPL (summarized from published reports)	Analytical method
			DL	PL	DL	PL	DL	DL			
<i>Physical parameters</i>											
pH	8.1 ± 0.49	7.1–8.8	6.5–8.5	24.39	24.39	6.5–8.5	24.39	24.39	24.39	Taste effects, mucus membrane	pH/EC/TDS meter
EC	762.8 ± 122.9	570–1058	–	Nil	Nil	Nil	1500	Nil	Nil	High-concentration laxative effect on human	pH/EC/TDS meter
TDS	488.2 ± 78.69	365 – 677	500	2000	39	Nil	1000	Nil	Nil	Gastrointestinal irritation	pH/EC/TDS meter
TH	214.1 ± 41.11	152.5 – 322.5	200	600	53.65	Nil	500	Nil	Nil	Calcification at arteries, gastrointestinal irritation	Calculation TH = 2.5*Ca ²⁺ +4.1*Mg ²⁺
TA	188.6 ± 34.49	112.3–262	200	600	39.02	Nil	Nil	Nil	Nil	Unpleasant taste	Titrimetric
<i>Major cations</i>											
Ca ²⁺	31.0 ± 10.11	15–59.3	75	200	Nil	Nil	300	Nil	Nil	May cause kidney and bladder problems and urination disorder	EDTA titration
Mg ²⁺	33.1 ± 9.33	21–62.3	30	100	61	Nil	100	Nil	Nil	Laxative effect	EDTA titration
Na ⁺	47.4 ± 15.07	22.4–86.1	–	–	–	–	200	Nil	Nil	High blood pressure	Flame photometric
K ⁺	12.7 ± 4.90	4.1–32.8	–	–	–	–	12	48.78	48.78	Bitter taste, laxative effects on human digestive and nervous system	Flame photometric
<i>Major anions</i>											
CO ₃ ²⁻	7.5 ± 8.36	0–28	–	–	–	–	–	–	–	Combined with Ca ²⁺ and Mg ²⁺ forms carbonate hardness	Titrimetric
HCO ₃ ⁻	214.7 ± 41.3	137–318	–	–	–	Nil	500	Nil	Nil		Titrimetric
NO ₃ ⁻	26.4 ± 19.57	2.4–80.6	45	NR	19.5	Nil	50	9.75	9.75	Methemoglobinemia in infants	Spectrophotometer
F ⁻	0.7 ± 0.41	0.0–2.0	1	1.5	19.5	4.8	1.5	4.8	4.8	Fluorosis, dental caries	Titrimetric
Cl ⁻	54.4 ± 30.11	21.3–179	250	1000	Nil	Nil	250	Nil	Nil	Injurious to people with heart and kidney ailment	Argentometric titration
SO ₄ ²⁻	45.1 ± 24.33	12–123.7	200	400	Nil	Nil	250	Nil	Nil	Gastrointestinal irritation along with Mg or Na, can have a cathartic effect on users	Spectrophotometer
PO ₄ ³⁻	0.1 ± 0.15	0.0–1.0	–	–	–	–	–	–	–		Titrimetric

All the parameters are measured in mg/L, except pH and EC

Table 3 Classification of groundwater based upon TDS (Davis and DeWiest 1967), TDS (Freeze and Cherry 1979) and TH (Sawyer and McCarty 1967)

TDS (mg/L)	Water classification/type	% of samples
<i>TDS (Davis and DeWiest 1967)</i>		
< 500	Desirable for drinking	61
500–1000	Permissible for drinking	39
1000–3000	Useful for irrigation	Nil
> 3000	Unfit for drinking and irrigation	Nil
TDS (mg/L)	Water classification/type	% of samples
<i>TDS (Freeze and Cherry 1979)</i>		
< 1000	Freshwater	100
1000–10,000	Brackish water	Nil
10,000–100,000	Saline water	Nil
> 100,000	Brine water	Nil
TH (as CaCO ₃ mg/L)	Water classification/type	% of samples
<i>TH (Sawyer and McCarty 1967)</i>		
< 75	Soft	Nil
75–150	Moderately hard	Nil
150–300	Hard	95
> 300	Very hard	5

were collected from each sampling stations. The groundwater samples were filtered through 0.45 µm Whatman filter paper using Millipore glass assembly unit and kept at a temperature of 4 °C until analysis. Another set of collected samples was acidified to pH ~ 2 by adding ultra-pure concentrated HNO₃ for measurements of the major cations. To avoid any oxidation process, containers were completely filled with groundwater to ensure that no air bubble be trapped within the sample. All the groundwater samples were analysed for major anions, viz. HCO₃⁻, CO₃²⁻, SO₄²⁻, PO₄³⁻, F⁻, Cl⁻ and NO₃⁻, and cations, viz. Ca²⁺, Mg²⁺, Na⁺ and K⁺, according to the standard methods enlisted in APHA (2005). ArcGIS 10.2.1 software developed by Environmental Systems Research Institute (ESRI) was used to prepare various maps. To know the spatial extent of various water quality parameters, inverse distance-weighted (IDW) algorithm interpolation method was used. In this technique of interpolation, unknown values of the pixels are estimated by averaging the known value. It is an effective algorithm extensively used in the mapping of spatial interpolation of groundwater quality parameters (Shakerkhatibi et al. 2019). The accuracy of the chemical ion data was examined using charge balance error (CBE) equation, and values were

within the acceptable limit of ± 5% (Hounslow 2018).

$$\text{CBE}\% = \frac{(\sum \text{Cations})\text{meq/L} - (\sum \text{Anions})\text{meq/L}}{(\sum \text{Cations})\text{meq/L} + (\sum \text{Anions})\text{meq/L}} * 100 \quad (1)$$

Procedure to evaluate drinking water quality index (DWQI)

DWQI estimation helps in determining the water quality suitability for drinking purpose by reducing a large water quality dataset into a single value (Yadav et al. 2018). DWQI is a very efficient method and an effective mathematical technique which provides information on the overall quality of water by examining every individual water parameters (Horton 1965; Herojeet et al. 2016). Weighted arithmetical index method developed by Horton (1965) was used to calculate DWQI. Ten water quality variables (pH, TDS, TH, Ca²⁺, Mg²⁺, HCO₃⁻, F⁻, Cl⁻, SO₄²⁻ and NO₃⁻) and Indian drinking water standards (BIS 2012; IS: 10500) were used for the estimation of DWQI. It was computed by adopting the following equation developed by Tiwari and Mishra (1985). Table 1

describes the relative weights of physicochemical parameters for DWQI calculation.

$$DWQI = \sum_{q_n} W_n / W_n \tag{2}$$

where W_n = unit weight of n th parameters is computed by using the following equation.

$$W_n = K / S_n \tag{3}$$

and K is the proportionality constant derived from

$$K = \left[1 / \left(\sum_{i=0}^n 1 / S_i \right) \right] \tag{4}$$

where S_n and S_i are the BIS standard values of the water quality parameter

$$q_{ni} = 100 \times [(V_a - V_i) / (V_s - V_i)] \tag{5}$$

q_{ni} is quality rating of i th parameter for a total of n water quality parameters, where V_a = actual value present in the water sample, V_i = ideal value (0 for all parameters except pH which is 7.0) and V_s = BIS standard value of water quality parameters.

Health risk assessment

Health risk assessment studies provide significant information about the chemical exposure from the groundwater quality, especially for drinking purpose (Wu and Sun 2016; Chen et al. 2017; Adimalla 2018; Adimalla and Li 2018; He and Wu 2018; He et al. 2018; Ahmed et al. 2019). Most of the groundwater samples have elevated concentration of NO_3^- and F^- , which may pose a serious health risk to humans. The conventional model established by the United States Environmental Protection Agency (USEPA 2009) was employed for the health risk assessment in the study area. Only non-carcinogenic pollutants (NO_3^- and F^-) were selected to perform the health risk assessment through oral pathway of exposure for the present study because other exposure pathways such as dermal and inhalation were negligible risk. Non-carcinogenic risk through ingestion is calculated as follows:

$$\begin{aligned} \text{Chronic Daily Intake (CDI)} \\ = (C \times IR \times ED \times EF) / (BW \times AT) \end{aligned} \tag{6}$$

$$HQ_{\text{ingestion}} = CDI / R_f D_{\text{ingestion}} \tag{7}$$

C = Concentration of contaminant in groundwater (mg/L); IR = ingestion rate of drinking water (L/d) (2 L/d for adults and 1 L/d for children); ED = exposure duration (years) (30 years and 12 years for adults and children, respectively); EF = exposure frequency (days/year) (365 days/year for both adults and children); BW = body weight of the receptor (kg) (60 kg for adults and 20 kg for children); and AT = average time (years) (10,950 days for adults and 4380 days for children);

Total non-carcinogenic health risks ($HI_{\text{ingestion}}$) due to ingestion exposure pathway (for NO_3^- and F^-) can be calculated as follows:

$$HI_{\text{ingestion}} = HQ_{\text{ingestion},NO_3^-} + HQ_{\text{ingestion},F^-} \tag{8}$$

$HQ_{\text{ingestion}}$ = hazard quotient of non-carcinogenic risk by ingestion pathway and $R_f D_{\text{ingestion}}$ = reference dosage for non-carcinogenic pollutant through drinking water exposure pathway. $R_f D_{\text{ingestion}}$ value for NO_3^- is 1.6 mg/(kg d) and for F^- is 0.06 mg/(kg d) is obtained from the Integrated Risk Information System (IRIS) database of the US EPA.

Chemometric techniques and graphical modelling

Chemometric analyses such as PCA and CA were employed to understand the sources of major ions and geochemical processes influencing the groundwater quality. These techniques have been widely used as unbiased methods for attaining important information from the hydrochemical dataset related to the groundwater system (Singh et al. 2004; Nagaraju et al. 2014; Mohamed et al. 2015; Herojeet et al. 2016, 2017; Li et al. 2018b; Rahman et al. 2018; Song et al. 2018). Varimax rotation with Kaiser normalization method was applied for the extraction of principal components (PCs). CA is a powerful data mining method, which classifies variables into clusters on the basis of similarities within a group and dissimilarities between different groups (Rajkumar et al. 2018). For cluster analysis, Ward’s method of linkage with squared Euclidean distance as a similarity measure approach was applied on water quality dataset (Otto 1998). Hydrogeochemical characterization of the groundwater was evaluated by Piper trilinear diagram using Geochemist’s Workbench Student Edition 12.0 software. Furthermore, saturation index (SI) of the groundwater was carried out using geochemical

Table 4 Water quality index classification

S. No.	DWQI	Class	No. of samples	% of samples
1	0–25	Excellent	5	12.20
2	26–50	Good	16	39.02
3	51–75	Poor	16	39.02
4	76–100	Very poor	3	7.32
5	> 100	Unfit for drinking	1	2.44

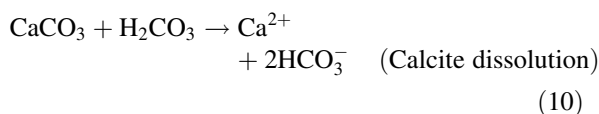
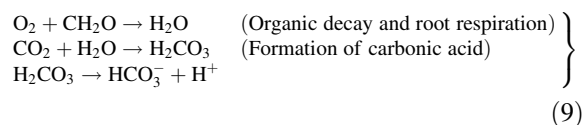
modelling technique PHREEQC. All the calculation, scatter plots and statistical analysis were performed by using the Microsoft Excel 2010, SPSS 16.0 and Minitab 17 softwares.

Results and discussion

General parameters of groundwater

The groundwater quality parameters of the study area such as maximum, minimum, mean and standard deviation and the concentration of each physicochemical parameters are compared with the standard values of the World Health Organization (WHO 2011) and the Bureau of Indian Standards (BIS 2012), respectively, for drinking water and are presented in Table 2. The analytical results of the physicochemical parameters are given in Supplementary Table 2. pH values range from 7.1 to 8.8 with mean \pm standard deviation (SD) of 8.1 ± 0.49 and indicate that the groundwater of the study area is slightly alkaline in nature. 24.39% samples have pH concentration above the permissible limit (6.5–8.5) of BIS (2012) and WHO (2011) (Table 2). The range and mean \pm SD of EC in the groundwater of the study area are $570 \mu\text{S}/\text{cm}$ to $1058 \mu\text{S}/\text{cm}$ and 762.8 ± 122.9 , respectively. The spatial distribution map of EC is shown in Supplementary Fig. 2(a). The entire groundwater samples are well within the permissible limit ($1500 \mu\text{S}/\text{cm}$) of WHO (2011) prescribed for drinking water. TDS and total hardness (TH) as CaCO_3 varied between 365 and 677 mg/L and 152.5 mg/L and 322.5 mg/L, and their spatial distribution map is presented in Supplementary Fig. 2(b and c), respectively. As per Davis and DeWiest (1967) classification of groundwater based on TDS, 39% samples of the study area are permissible for drinking (Table 3). Also, TDS value is found below 1000 mg/l in all the samples and indicates that the groundwater is fresh in nature as per Freeze and

Cherry (1979) classification (Table 3). According to Sawyer and McCarty (1967) based on TH, 95% of the groundwater samples fall under hard water category and the remaining 5% samples fall under very hard water category (Table 3). 44% of total alkalinity (TA) of samples is beyond the desirable limits (200 mg/L) of BIS (2012) and WHO (2011) (Table 3) and its spatial distribution map is shown in Supplementary Fig. 2(d). Weathering of silicate such as feldspar and dissolution of carbonate minerals in the presence of soil CO_2 (g) is responsible for the high alkalinity by releasing HCO_3^- and Na^+ ions in the groundwater as expressed in Eqs. 9, 10 and 14 (Keesari et al. 2016a; Roy et al. 2018). In the top soil, decaying of humus (CH_2O) along with root respiration significantly increases the amount of soil CO_2 (g). Thus, the infiltrating H_2O through the top soil react with soil CO_2 and leads to the formation of carbonic acid (H_2CO_3). The breakdown of H_2CO_3 in the presence of excess H_2O releases HCO_3^- ion in the aquifer (Raju and Singh 2017) as expressed in Eq. 9.



Major cations and anions in the groundwater

Abundance order of the major ions in the groundwater samples is $\text{Na}^+ > \text{Mg}^{2+} > \text{Ca}^{2+} > \text{K}^+$ and $\text{HCO}_3^- > \text{Cl}^- > \text{SO}_4^{2-} > \text{NO}_3^- > \text{CO}_3^{2-} > \text{F}^- > \text{PO}_4^{3-}$, respectively, for both cations and anions (Fig. 4a, b). The concentration of Ca^{2+} and Mg^{2+} in study area ranged from 15.0 to 59.3 mg/L and 21.0 mg/L to 62.3 mg/L with mean \pm SD of 31.1 ± 10.10 and

Table 5 Calculated non-carcinogenic health risk for adults and children

ID	For adults			For children		
	HQ (NO ₃ ⁻)	HQ (F ⁻)	HI _{ingestion} (Total)	HQ (NO ₃ ⁻)	HQ (F ⁻)	HI _{ingestion} (Total)
J1	0.67	0.24	0.91	1.00	0.37	1.37
J2	0.94	0.37	1.31	1.41	0.55	1.96
J3	0.28	0.22	0.50	0.41	0.33	0.75
J4	0.14	0.23	0.37	0.22	0.34	0.56
J5	0.69	0.92	1.61	1.03	1.38	2.42
J6	0.16	0.31	0.47	0.23	0.47	0.70
J7	0.38	0.42	0.80	0.56	0.63	1.20
J8	1.68	0.56	2.23	2.52	0.83	3.35
J9	0.59	0.23	0.83	0.89	0.35	1.24
J10	0.44	0.24	0.68	0.66	0.36	1.01
J11	0.19	0.27	0.46	0.28	0.40	0.68
J12	0.21	0.26	0.47	0.32	0.39	0.71
J13	0.32	0.48	0.80	0.48	0.73	1.20
J14	0.71	0.43	1.14	1.06	0.65	1.71
J15	0.61	0.49	1.11	0.92	0.74	1.66
J16	1.60	0.51	2.11	2.40	0.77	3.17
J17	0.36	0.49	0.85	0.54	0.74	1.28
J18	0.35	0.39	0.74	0.53	0.58	1.11
J19	0.27	0.83	1.10	0.41	1.24	1.65
J20	0.52	0.52	1.04	0.78	0.78	1.55
J21	0.55	0.51	1.05	0.82	0.76	1.58
J22	0.18	0.59	0.77	0.27	0.89	1.16
J23	0.77	0.36	1.13	1.15	0.54	1.69
J24	0.11	1.09	1.20	0.17	1.63	1.81
J25	0.31	0.34	0.65	0.46	0.52	0.98
J26	0.34	0.31	0.65	0.51	0.47	0.98
J27	0.79	0.58	1.36	1.18	0.87	2.04
J28	1.04	0.56	1.60	1.57	0.84	2.41
J29	1.04	0.02	1.05	1.55	0.03	1.58
J30	1.15	0.62	1.78	1.73	0.93	2.66
J31	0.49	0.26	0.75	0.74	0.38	1.12
J32	1.34	0.54	1.88	2.01	0.82	2.82
J33	0.96	0.55	1.51	1.45	0.83	2.27
J34	0.67	0.48	1.15	1.01	0.72	1.72
J35	0.12	0.02	0.13	0.18	0.03	0.20
J36	0.14	0.18	0.31	0.20	0.27	0.47
J37	0.05	0.03	0.08	0.08	0.04	0.12
J38	0.73	0.56	1.29	1.10	0.84	1.94
J39	0.33	0.32	0.65	0.50	0.48	0.98
J40	0.14	0.28	0.43	0.21	0.43	0.64
J41	0.21	0.08	0.29	0.31	0.13	0.44
Min	0.05	0.02	0.08	0.08	0.03	0.12
Max	1.68	1.09	2.23	2.52	1.63	3.35

Table 5 continued

ID	For adults			For children		
	HQ (NO ₃ ⁻)	HQ (F ⁻)	HI _{ingestion} (Total)	HQ (NO ₃ ⁻)	HQ (F ⁻)	HI _{ingestion} (Total)
Mean	0.55	0.41	0.96	0.83	0.61	1.44

33.1 ± 9.3, respectively (Table 2). Dissolved magnesium exceeds calcium in aquifers once calcium precipitates after reaching supersaturation and accounts for higher magnesium concentrations than calcium (Hem 1985). Therefore, 61% of groundwater samples have Mg²⁺ contents above the desirable limit (30 mg/L) of BIS (2012), which may contribute to total hardness in groundwater (Table 2). The higher content of Mg²⁺ in the groundwater of the study area may be due to weathering of dolomite minerals, sandstone and applications of chemical fertilizers and pesticides as most of the sampling locations are from the cultivated land (Keesari et al. 2014). The spatial distribution map of Ca²⁺ and Mg²⁺ is given in Supplementary Fig. 2(e) and (f), respectively. Na²⁺ in the study area ranged from 22.4 to 86.1 mg/L (mean ± SD of 47.4 ± 15.07) and most dominant cation in groundwater (Fig. 4a). The concentration of K⁺ in the study area ranged from 4.1 to 32.8 mg/L with 51% samples above the permissible limit (12 mg/L) of WHO (2011) (Table 2). The source of Na⁺ and K⁺ in the study area may be due to weathering of potash and silicate minerals, application of potash fertilizers and sewage wastewater (Srinivasamoorthy et al. 2014). The spatial distribution map of Na⁺ and K⁺ is presented in Supplementary Fig. 2(g and h).

Among the anions, HCO₃⁻ is the dominant anion (Fig. 4b), ranging from 137.0 to 318.0 mg/L (mean ± SD of 214.7 ± 41.3), and their spatial distribution map of HCO₃⁻ is shown in Supplementary Fig. 2(i). The concentration of CO₃²⁻ ranges from 0.0 to 28.0 mg/L with mean ± SD of 7.5 ± 8.3. The presence of HCO₃⁻ and CO₃²⁻ ions is mostly responsible for the alkalinity of groundwater. Major source of HCO₃⁻ ion in the groundwater is silicate weathering and dissolution of carbonate rocks such as calcite [CaCO₃] and dolomite [CaMg(CO₃)₂] in the aquifers (Keesari et al. 2014) and discussed in Eqs. 10 and 18. NO₃⁻ concentration varied from 2.4 to 80.6 mg/L (mean ± SD of 26.4 ± 19.57), and about 20% and 12% groundwater samples have exceeded the

permissible limits for NO₃⁻ in drinking water of BIS (2012) and WHO (2011), respectively [Table 2 and Supplementary Fig. 26(j)]. The consumption of water with high NO₃⁻ content causes blue baby or methemoglobinemia in infants, and gastric cancer, central nervous system birth defects and hypertension in adults (WHO 1997; Yadav et al. 2018). Anthropogenic activities such as application of fertilizers, domestic and municipal sewage and seepage from the septic tanks are the main sources of nitrate in the study area (Keesari et al. 2016a; Raju and Singh 2017). According to the Adimalla et al. 2018 classification, around 20% samples show high health risk due to excess content of NO₃⁻ Supplementary Table 3. F⁻ content in the study area varied from 0.03 mg/L to 2.0 mg/L with mean ± SD value of 0.7 ± 0.40. Nearly 20% and 5% samples have F⁻ concentration above the desirable and permissible limits of BIS (2012) [Table 2 and Supplementary Fig. 2(k)]. As per Adimalla et al. 2018 classification, around 5% samples show dental fluorosis risk and 63.4% samples have F⁻ content between 0.6 and 1.5 mg/L, which indicates human health risk (Supplementary Table 3). Several conditions such as alkaline pH, higher content of HCO₃⁻ and lower concentrations of Ca²⁺ in the groundwater of the study area provide favourable conditions for F⁻ enrichment in the aquifer. Apart from natural sources, some anthropogenic sources such as industrial activities like brick kiln and seepage of untreated sewage water may be the reason for the elevated concentration of fluoride in the study area (Roy et al. 2018; Yadav et al. 2018). The concentration of SO₄²⁻ and Cl⁻ in study area varied from 12.0 to 123.7 mg/L and 21.3 mg/L to 179.0 mg/L, respectively, and within the BIS (2011) and WHO (2011) (Table 2). Sodalite, micas and apatite are the chief minerals that contribute chloride to groundwater (Karanth 1987). Oxidation of sulphide minerals, weathering of rocks containing gypsum (CaSO₄·2H₂O) mineral and anthropogenic input like industrial effluent, fertilizers may contribute to SO₄²⁻ in the

Table 6 Hydrochemical facies of the groundwater of the study area derived from piper diagram

Class	Groundwater types of corresponding subdivisions of facies	No. of samples	% of samples
I	Ca ²⁺ –Mg ²⁺ –Cl [–] –SO ₄ ^{2–}	3	7.31
II	Na ⁺ –K ⁺ –Cl [–] –SO ₄ ^{2–}	Nil	Nil
III	Na ⁺ –K ⁺ –HCO ₃ [–]	2	4.87
IV	Ca ²⁺ –Mg ²⁺ –HCO ₃ [–]	36	87.80
1	Alkaline earths (Ca ²⁺ –Mg ²⁺) exceed alkalies (Na ⁺ –K ⁺)	39	95.12
2	Alkalies exceed alkaline earths	2	4.87
3	Weak acids (HCO ₃ [–] –CO ₃ ^{2–}) exceed strong acids (Cl [–] –SO ₄ ^{2–} –F [–])	38	92.62
4	Strong acids exceed weak acids	3	7.31
5	Ca ²⁺ –Mg ²⁺ and HCO ₃ [–] –CO ₃ ^{2–} (temporary hardness); magnesium bicarbonate type (carbonate hardness (secondary alkalinity) exceeds 50%)	36	87.80
6	Ca ²⁺ –Mg ²⁺ and Cl [–] –SO ₄ ^{2–} (permanent hardness); calcium chloride type (non-carbonate hardness (secondary salinity) exceeds 50%)	3	7.31
7	Cl [–] –SO ₄ ^{2–} and Na ⁺ –K ⁺ (saline); sodium chloride type (non-carbonate alkali (primary salinity) exceeds 50%)	Nil	Nil
8	HCO ₃ [–] –CO ₃ ^{2–} and Na ⁺ –K ⁺ (alkali carbonate); sodium bicarbonate type (carbonate alkali (primary alkalinity) exceeds 50%)	2	4.87
9	None of the cation and anion pairs exceed 50%	5	12.19
A	Calcium type	Nil	Nil
B	No dominant (cations)	36	87.80
C	Magnesium type	5	12.19
D	Sodium type	Nil	Nil
E	Bicarbonate type	38	92.62
B	No dominant (anions)	2	4.87
F	Sulphate type	Nil	Nil
G	Chloride type	1	2.43

groundwater (Roy et al. 2018). The spatial distribution map of Cl[–] is presented in Supplementary Fig. 2(I). The concentration of PO₄^{3–} in the study area is quite low, ranged from 0.00 to 1.0 mg/L (Table 3). However, BIS (2012) and WHO (2011) have not suggested any guideline limits for PO₄^{3–} ion in the groundwater.

Drinking water quality index evaluation

The computed DWQI values of groundwater of Jalandhar district varied from 6 to 117 with mean value 50.3, as shown in Supplementary Table 4. Spatial distribution map of the DWQI is shown in Fig. 5. According to the classification of DWQI (Tiwari and Mishra 1985), majority of the samples fall under ‘excellent to good’, followed by ‘poor to very poor’ and ‘unfit for drinking’ classes for drinking

purposes, with values of 51%, 46% and 3%, respectively (Table 4). Extensive agricultural, indiscriminate use of chemical fertilizers, industrial activities and discharge of untreated sewage water may be responsible for groundwater quality degradation (Keesari et al. 2014). The south-western and central parts of the study area show more deteriorated water quality in comparison with the northern part (Fig. 5). One groundwater sample location (J24) that requires urgent attention is falling under ‘unfit for drinking category’. Continuous consumption of groundwater for drinking purpose from this pocket may pose a great threat to human health, and thus, immediate measure is must in such areas. As per the groundwater elevation map (Fig. 3), the aquifer flow direction is towards the south-west which is another key factor for accumulating the contaminants dispersing from northern and

Table 7 Principal component matrix of the groundwater after varimax rotation with Kaiser normalization

Rotated principal component matrix						
Variable	PC1	PC2	PC3	PC4	PC5	Communality
pH	0.07	0.15	– 0.85	0.24	– 0.07	0.816
EC	0.60	0.73	0.23	0.02	0.20	0.983
TDS	0.60	0.73	0.23	0.02	0.20	0.983
TA	– 0.01	0.88	– 0.36	– 0.04	0.07	0.919
TH	0.86	0.23	– 0.06	– 0.22	0.31	0.945
Ca ²⁺	0.07	0.14	0.07	– 0.03	0.95	0.939
Mg ²⁺	0.88	0.15	– 0.11	– 0.22	– 0.29	0.937
Na ⁺	0.11	0.63	0.41	0.49	– 0.07	0.818
K ⁺	0.29	0.14	0.68	0.25	0.20	0.658
HCO ₃ [–]	0.00	0.90	– 0.06	– 0.23	0.02	0.86
CO ₃ ^{2–}	– 0.01	0.01	– 0.75	0.44	0.13	0.774
NO ₃ [–]	0.71	– 0.17	0.08	0.44	0.05	0.731
F [–]	– 0.06	0.06	– 0.06	0.79	0.07	0.632
Cl [–]	0.77	0.11	0.39	0.26	0.10	0.839
PO ₄ ^{3–}	0.45	– 0.04	0.52	0.19	0.42	0.68
SO ₄ ^{2–}	– 0.09	0.29	0.19	– 0.64	0.10	0.547
Eigenvalue	5.29	2.72	2.248	1.656	1.147	
% of Variance	33.1	17.0	14.1	10.3	7.2	
Cumulative Variance (%)	33.1	50.1	64.2	74.5	81.7	
Source	Mixed factor (dissolution of dolomite and cation exchange and application of fertilizer, irrigation return flow and domestic sewage)	Natural factor (silicate and carbonate (CaCO ₃) weathering and the dissolution of calcite, dolomite, halite and albite minerals)	Mixed factor (carbonate weathering and application of potash fertilizers and agrochemicals)	Mixed factor (aquifer materials interaction and fertilizers by-products)	Natural factor [dissolution of calcite and limestone (kankars) along with the cation exchange process]	

Significant factor loadings are boldfaced

Moderately significant factor loadings are in bolditalics

eastern region besides local or nearby pollution sources. The result of DWQI is well corroborated with groundwater movement, which indicates that regular and strict monitoring of groundwater is a necessity in the south-western part and certain pockets to prevent further contamination. Effective pollution control measures would significantly reduce overall pollution, which further improves the quality of water, and people depend on such water source.

Health risk assessment

The results of the non-carcinogenic risk assessment for HQ_{ingestion} and HI_{ingestion} are summarized in Table 5. The HQ_{ingestion} (NO₃[–]) ranges from 0.08 to 2.52 and 0.05 to 1.68 with a mean value of 0.83 and 0.55 for children and adults (Table 5). About 36.58% and 14.6% groundwater samples show HQ > 1 for children and adults, respectively, and suggest that drinking groundwater polluted with NO₃[–] could pose severe health hazard to children than adults. Similarly,

Table 8 Clustering pattern of groundwater samples in the study area

Parameters	C1 [(n = 23) (1,38,2,37,36,39,40,41,3,6,20,12,4,11,35,27,26,23,15,33,21,34)]	C2 [(n = 9) (7,22,10,24,14,25,17,18,19)]	C3[(n = 8) (5,9,8,16,28,29,31,30)]	C4 [(n = 1) (32)]
pH	7.9	8.5	8.3	7.1
EC	734.6	672.4	909.5	1050.0
TDS	470.1	430.4	582.1	672.0
TH	201.5	186.6	270.1	301.6
TA	179.7	193.4	213.5	148.4
Ca ²⁺	29.8	30.0	32.7	54.7
Mg ²⁺	30.8	27.1	45.7	40.0
Na ⁺	46.0	42.8	53.4	72.3
K ⁺	12.6	9.8	13.8	32.8
HCO ₃ ⁻	213.2	199.2	240.5	181.0
CO ₃ ⁻	3.0	18.0	9.8	0.0
NO ₃ ⁻	20.5	16.5	49.7	64.2
F ⁻	0.60	0.97	0.83	0.98
Cl ⁻	46.5	37.4	80.7	179.0
PO ₄ ³⁻	0.04	0.03	0.05	1.00
SO ₄ ²⁻	52.1	33.5	39.9	31.0

Bold indicates maximum mean values

Bold italics indicates higher mean values

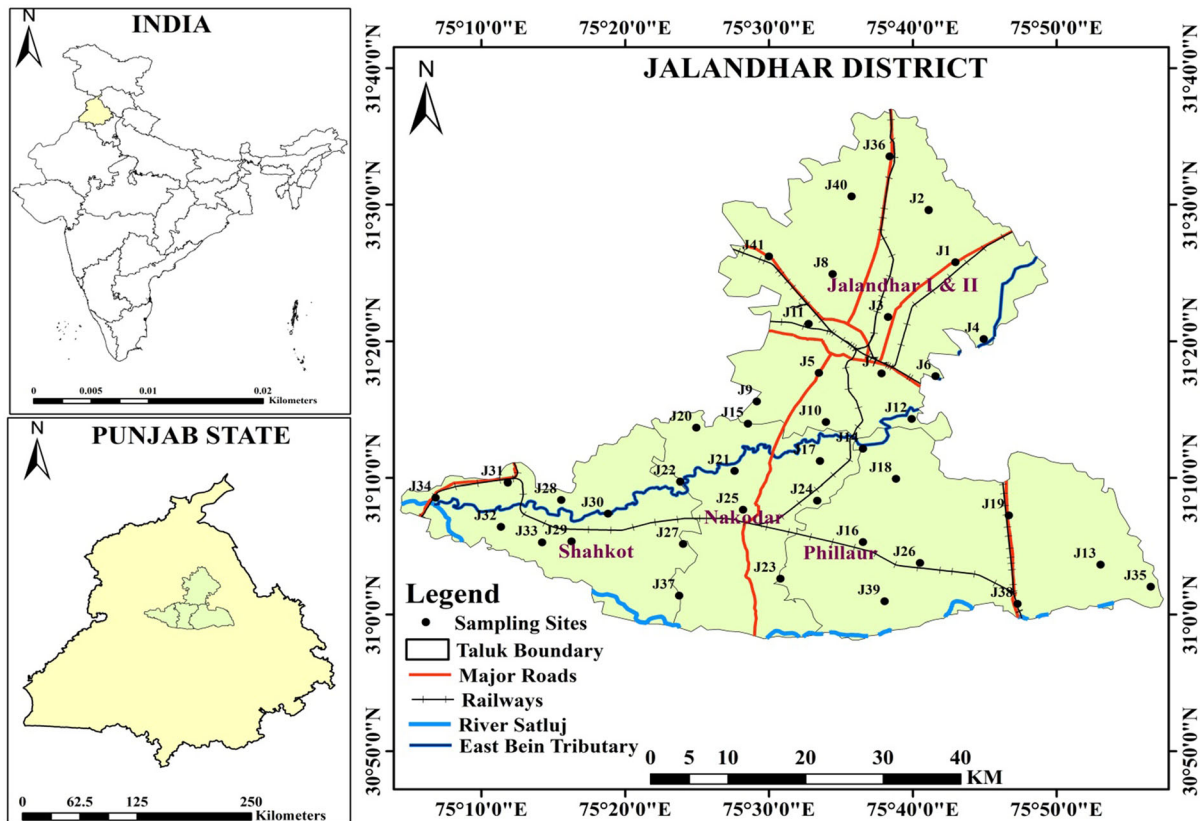


Fig. 1 Map of the study area with groundwater sampling locations

$HQ_{\text{ingestion}} (F^-)$ for children and adults varied between 0.03 and 1.63 and 0.02 and 1.09 with 7.32% and 2.4% samples showing $HQ > 1$. The results of $HQ_{\text{ingestion}}$ (Table 5 and Fig. 6) indicate that children and adults are more vulnerable to NO_3^- than F^- contaminants in drinking water. Further, compared with adults, the non-carcinogenic risk of NO_3^- is much more serious for children. HI more than 1 indicates a potential non-carcinogenic effect on human health, while $HI < 1$ indicates negligible risk on human health. For adults, the calculated $HI_{\text{ingestion}} (NO_3^- \text{ and } F^-)$ is varied from 0.08 to 2.23 with mean value of 0.96, and 19 (46.34%) groundwater samples have shown $HI > 1$. The calculated $HI_{\text{ingestion}} (NO_3^- \text{ and } F^-)$ for children is varied from 0.12 to 3.35 with approximately 68% (28 groundwater samples) samples showing $HI > 1$. The mean value of $HI_{\text{ingestion}}$ for children (1.44) is higher than 1, inferring that the children are more prone to the non-carcinogenic health risk from NO_3^- and F^- . Thus, the health risk assessment for HQ and HI

confirmed that children are more vulnerable and threatening as compared to the adults and cannot be ignored. Overall the population of the area under investigation are at high non-carcinogenic health risk and more people may become prone to disease in the future.

Evaluation of groundwater salinization

Revelle index (1941)

Revelle index (1941) is used for the evaluation of the degree of groundwater salinization in the study area and calculated by using Eq. 11. It has been considered to be an effective method for groundwater salinization evaluation in arid and semi-arid regions (Revelle 1941).

$$\text{Revelle index (RI)} = \text{Cl}^- / (\text{HCO}_3^- + \text{CO}_3^{2-}) \quad (11)$$

where all the values are in meq/L

The RI value varies from 0.1 to 1.5 meq/L in the study area (Supplementary Table 7). As per the classification based on RI values, 78% of the groundwater samples in the study area are not affected by salinization (RI value < 0.5 meq/L) and 22% samples are slightly influenced by salinity (Supplementary Table 5). Figure 7 shows that groundwater salinization is more prominent in the south-western part and few pockets in the south and central parts of the study area. It may be due to anthropogenic activities such as uncontrolled agricultural practices, seepage from municipal sewage and septic tanks and aquifer movement in the study area. Therefore, groundwater movement is also towards the south-western direction (Fig. 3) and this area is more affected by salinization problem and poor water quality as per the Revelle index and DWQI map (Fig. 5). As we discussed earlier that aquifer movement is also a key responsible factor complying the accumulation of ions along the flow path, thereby affecting the water quality (Fig. 3). The results of RI and DWQI draw the clear picture that poor water quality in the south-western and some parts of the study area is influenced by groundwater

movement leading to salinization besides local pollution sources. Hence, it is recommended that the water quality study of an area shall be assessed together with RI and groundwater movement. This integrative study is a noble approach to understand groundwater quality and salinity related to flow direction and help to demarcate the aquifer region for immediate restoration and management formulation and policy as well.

Mechanisms controlling groundwater chemistry

Gibbs diagram and water–rock interaction

To understand the mechanisms controlling groundwater chemistry in the alluvial aquifer of Jalandhar district, water quality data were plotted in the Gibbs diagrams (Gibbs 1970). Figure 8 depicts that majority of the groundwater samples clustered on the rock dominance zone, suggesting that geochemical processes such as percolating rock–water interactions and chemical solute exchange processes of rock-forming minerals influence the hydrochemistry. Further, Schoeller indices or chloro-alkaline indices (Schoeller

Fig. 2 LULC map of the Jalandhar district

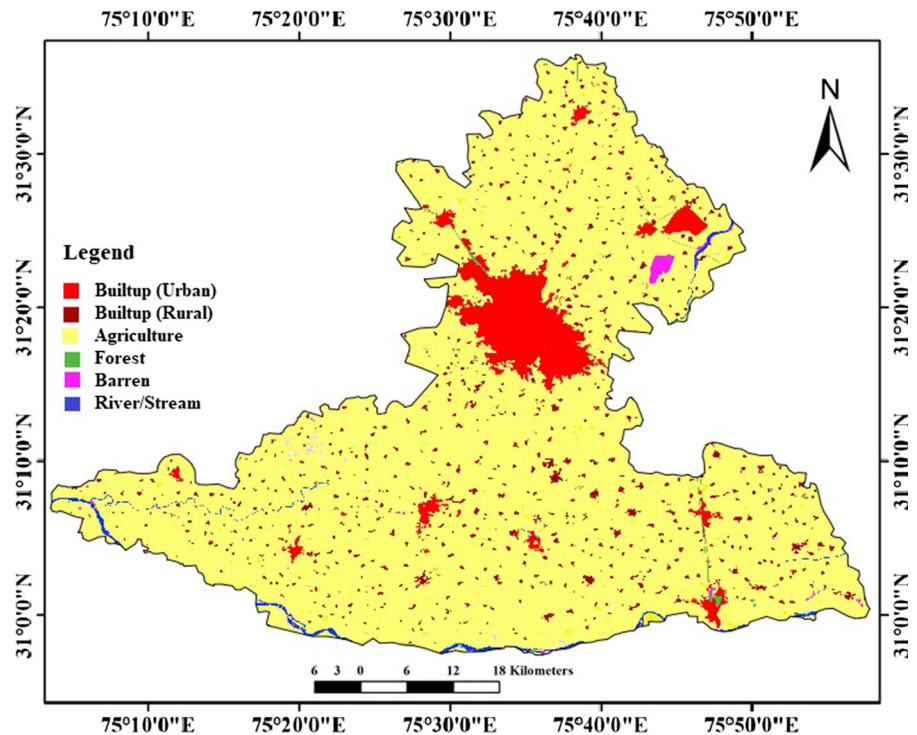
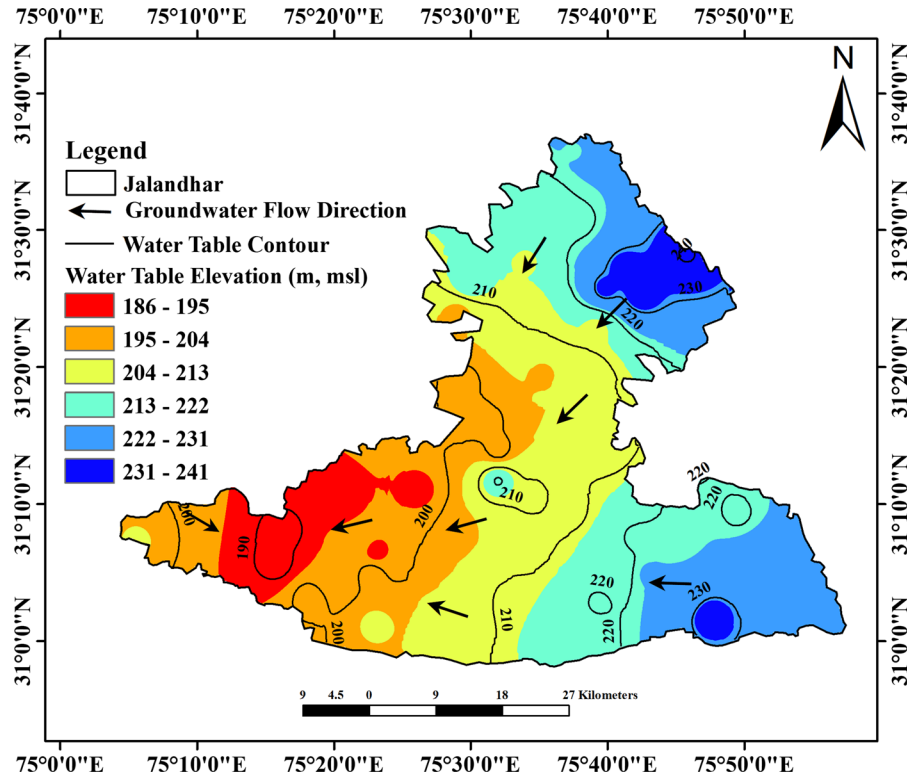


Fig. 3 Groundwater flow direction in the study area



1967) were employed to assess the ion exchange reactions among the host rocks and aquifer during their residence time and evaluated by Eqs. 12 and 13.

$$CAI - I = \frac{Cl^- - (Na^+ + K^+)}{Cl^-} \quad (12)$$

$$CAI - II = \frac{Cl^- - (Na^+ + K^+)}{(SO_4^{2-} + HCO_3^- + CO_3^{2-} + NO_3^-)} \quad (13)$$

The positive and negative values of CAI-I and CAI-II explain reverse ion exchange reaction and chloro-alkaline disequilibrium (cation exchange),

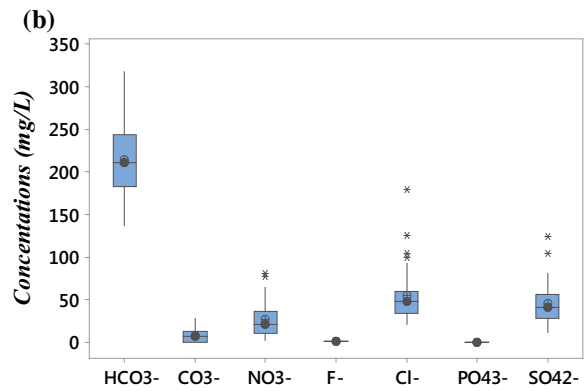
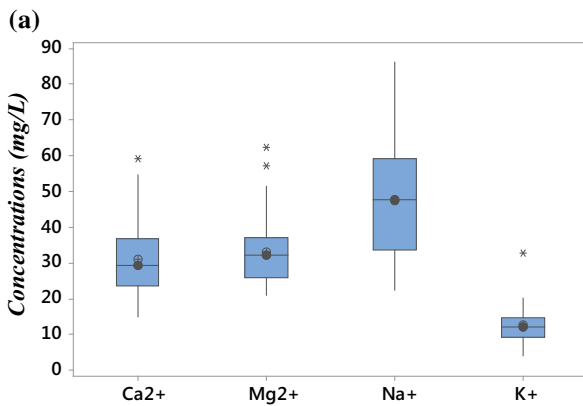


Fig. 4 a and b Box plots of the major cations and anions of groundwater of the study area (asterisk: outlier, cross dot: mean, whisker horizontal line: median, whisker vertical line: maximum and minimum and box: first quartile and third quartile)

Fig. 5 Spatial distribution map of the DWQI

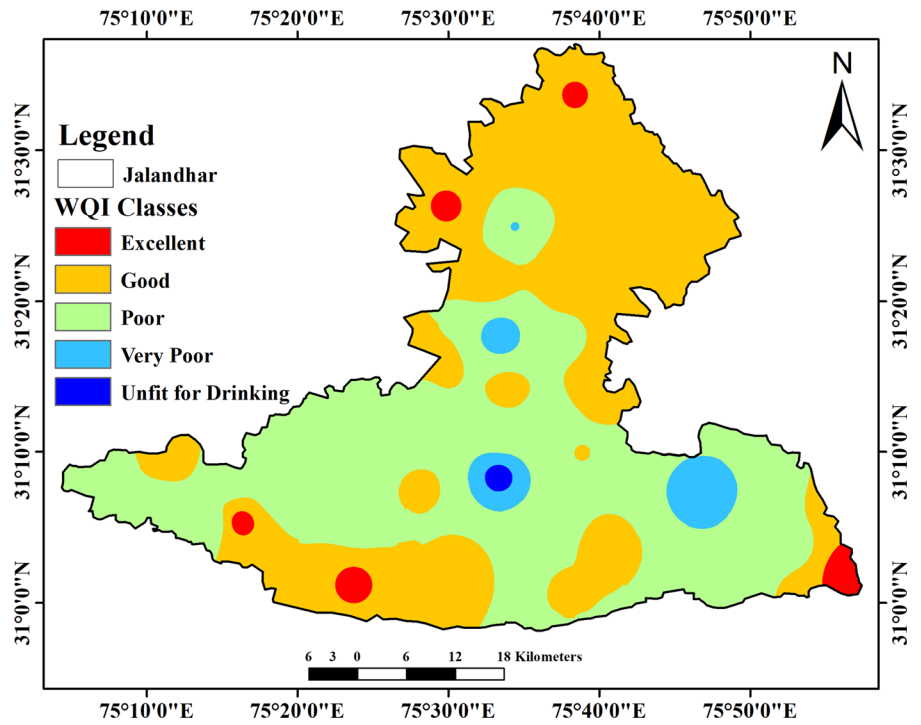


Fig. 6 Health risk assessment for adults and children

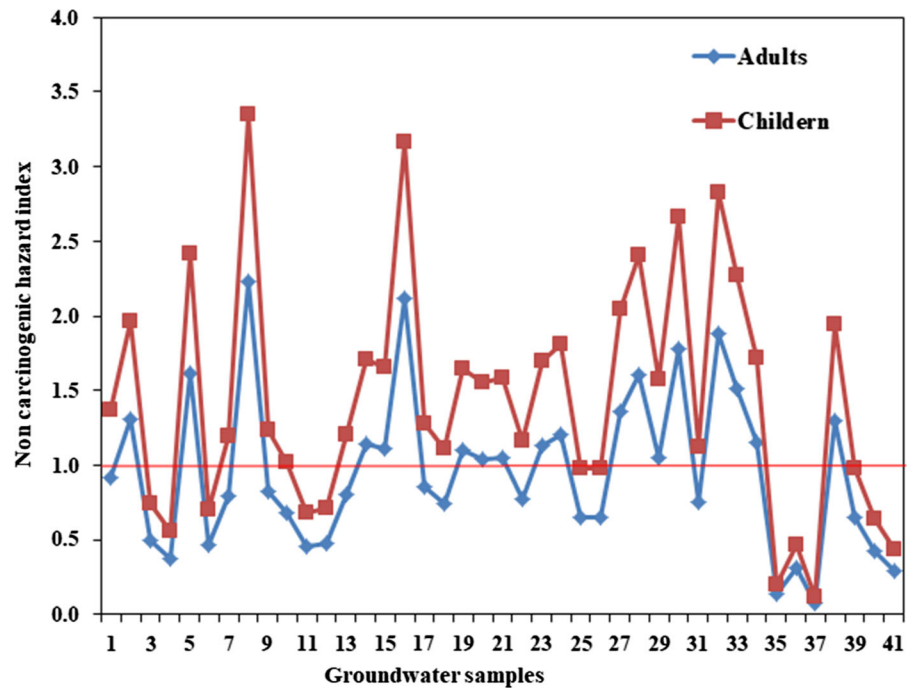
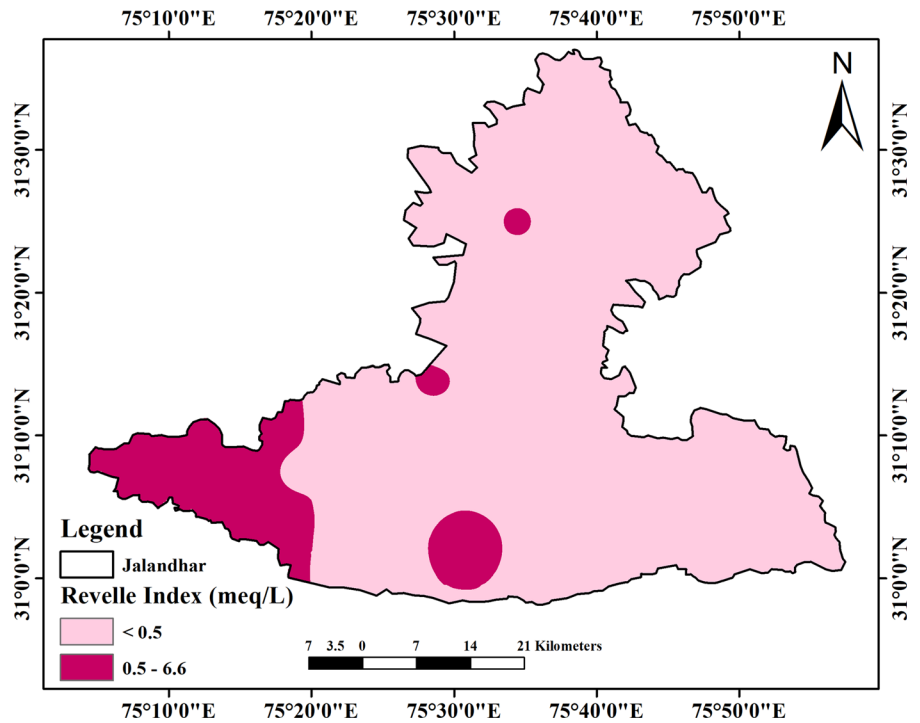


Fig. 7 Spatial distribution map of the groundwater salinization



respectively. 90% groundwater samples exhibit negative ratio for both CAI-I and CAI-II indices, indicating the chloro-alkaline disequilibrium or dominance of cation exchange process in the aquifer system (Supplementary Table 7 and Supplementary Fig. 3). In this process, Ca^{2+} and Mg^{2+} ions in the groundwater are exchanged with Na^+ and K^+ of the host rock

as shown in Eq. 14 (Rajmohan and Elango 2003), whereas only 10% of the samples showed positive values illustrating the base exchange reaction (Supplementary Table 7 and Supplementary Fig. 3).

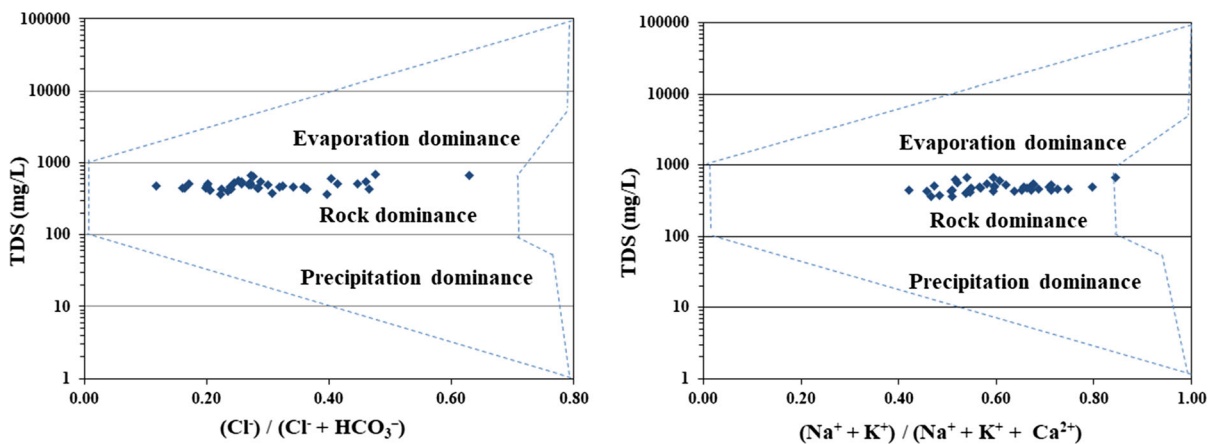
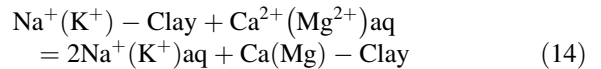


Fig. 8 Gibbs diagram representing controlling factors of groundwater quality

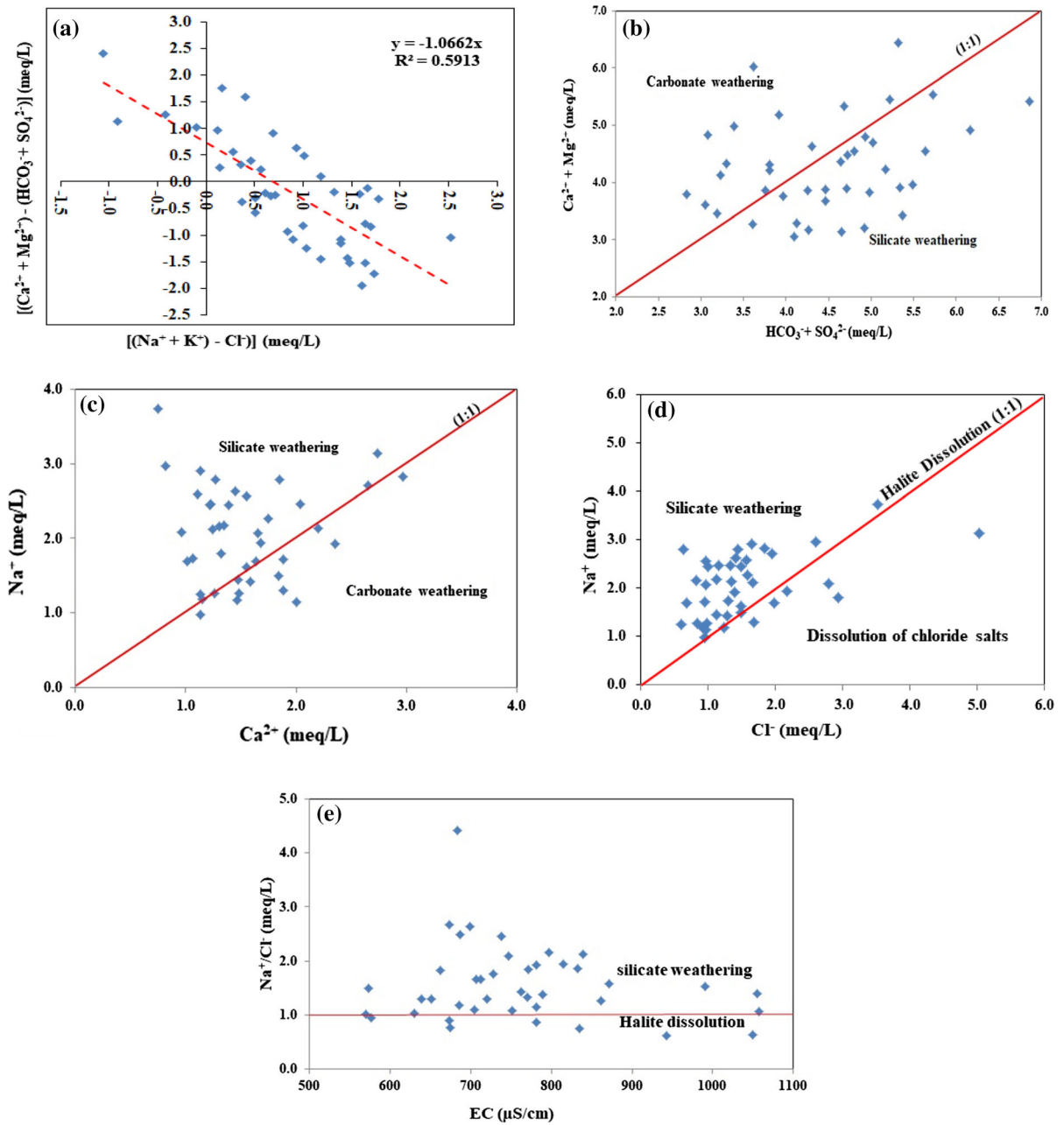


Fig. 9 Major ion relationship: **a** $(Ca^{2+} + Mg^{2+}) - (HCO_3^{-} + SO_4^{2-})$ versus $(Na^{+} + K^{+} - Cl^{-})$, **b** $Ca^{2+} + Mg^{2+}$ versus $HCO_3^{-} + SO_4^{2-}$, **c** Na^{+} versus Ca^{2+} , **d** Na^{+} versus Cl^{-} , **e** Na^{+}/Cl^{-} versus EC, **f** Ca^{2+}/Na^{+} versus HCO_3^{-}/Na^{+} , **g** Ca^{2+}/Na^{+}

versus Mg^{2+}/Na^{+} , **h** SO_4^{2-} versus Ca^{2+} , **i** Ca^{2+}/Mg^{2+} versus Samples, **j** $Ca^{2+} + Mg^{2+}$ versus TZ^{+} , **k** $Na^{+} + K^{+}$ versus TZ^{+} for groundwater in the study area

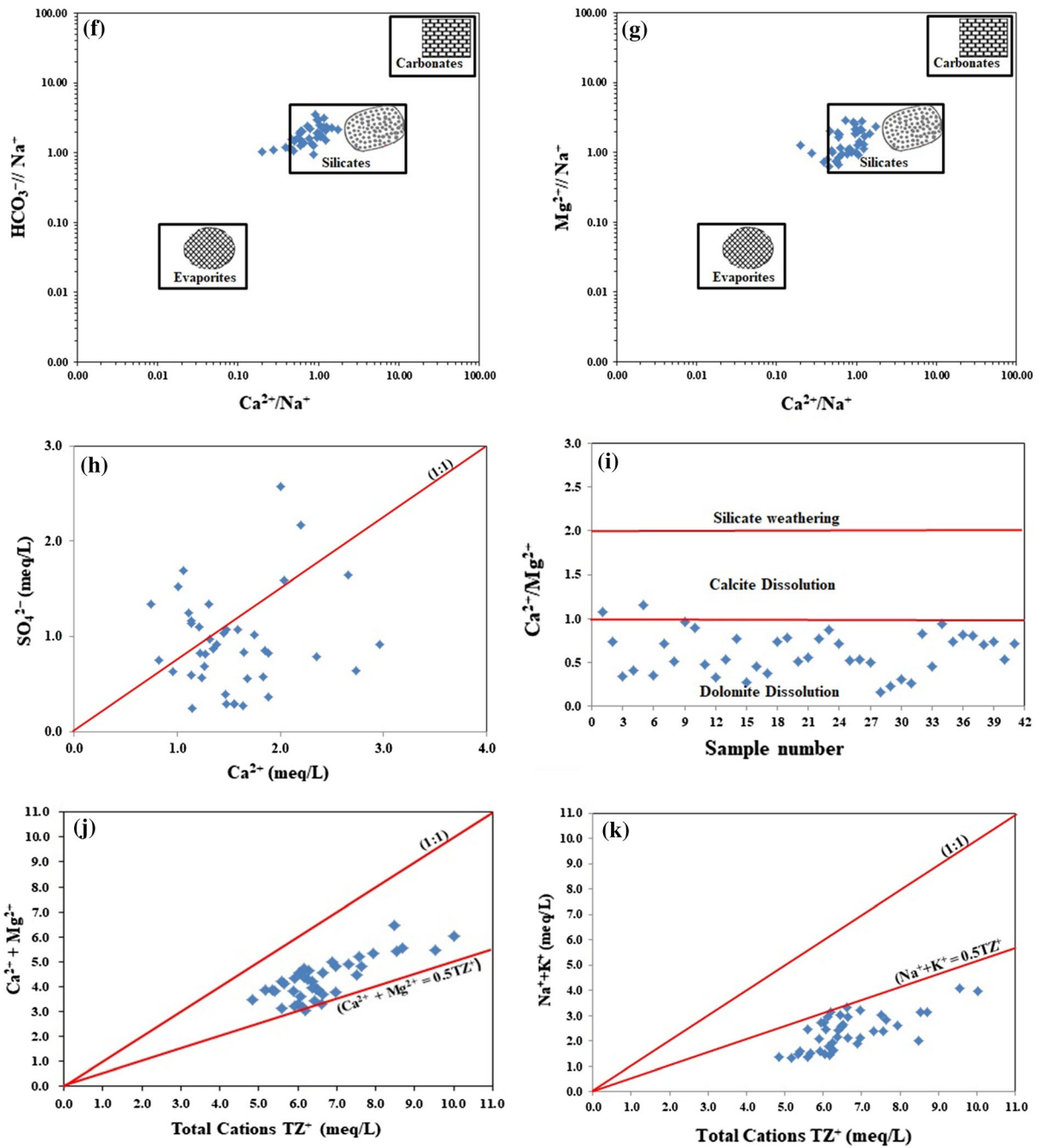


Fig. 9 continued

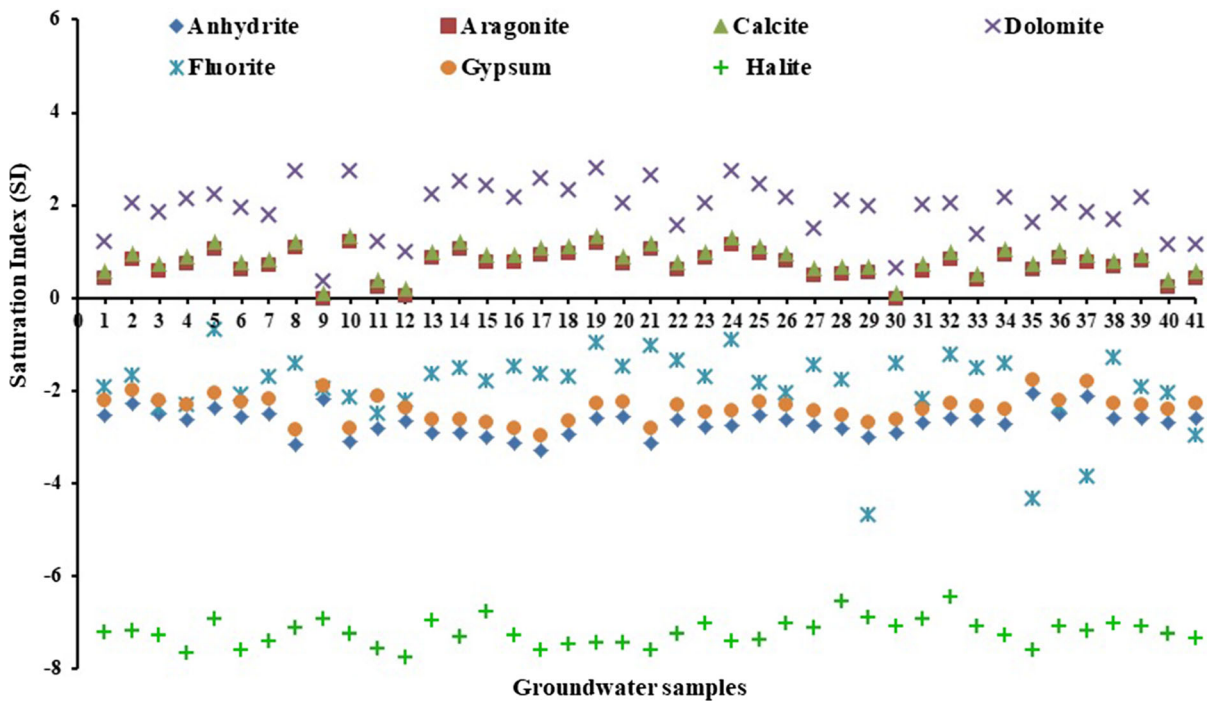
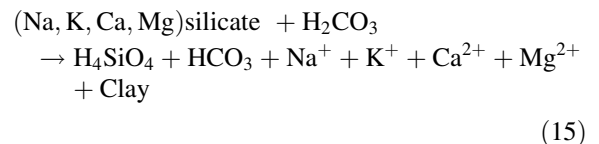


Fig. 10 Saturation index of the groundwater of the study area

Weathering processes

The concentration of dissolved minerals or major ions in the groundwater is mainly due to various direct and indirect interactions between aquifer and host rock. Various bivariate plots were prepared to understand the chemical weathering profile and sources of solutes in the alluvial aquifer. The cation exchange processes involved in the aquifer is further substantiated by the scatter plot between $[(Ca^{2+} + Mg^{2+}) - (HCO_3^- + SO_4^{2-})]$ and $[(Na^+ + K^+) - Cl^-]$. The majority of the groundwater samples fall on a slope of -1 [slope $y = -1.0662x$, Fig. 9a] and clearly indicate the ion exchange process between Ca^{2+} , Mg^{2+} and Na^+ ions in the alluvial aquifer of the study area (Keesari et al. 2016a; Batabyal and Gupta 2017). The scatter plot between $Ca^{2+} + Mg^{2+}$ and $HCO_3^- + SO_4^{2-}$ (Fig. 9b) revealed that both carbonate and silicate mineral dissolutions are affecting the aquifer chemistry in the study area. The groundwater samples (36%) were above the equiline (1:1), reflecting reverse ion process, and about 61% samples were below the equiline (1:1), suggesting ion exchange is occurring in the region (G et al. 2015; Liao et al. 2018). One

groundwater sample (3%) falls on equiline (1:1) and is influenced by the dissolution of calcite and dolomite in the alluvial aquifer (Singh et al. 2017). The general silicate weathering reaction with carbonic acid (Das and Kaur 2001) is given in Eq. 15.



The ion exchange process is further validated by Na^+ versus Ca^{2+} plot (Fig. 9c), as the majority of the groundwater samples fall above and close to the equiline (1:1), suggesting the prevalence of ion exchange process in the study area (Singh et al. 2018). The scatter plot between Na^+ vs Cl^- is used to identify the sources of salinity and saline incursions in arid and semi-arid regions (Gaofeng et al. 2010). Figure 9d depicts that majority of the groundwater samples fall above the equiline (1:1) and signify that Na^+ may be attributed to silicate weathering (weathering of albite as expressed in Eq. 16) and cation exchange (Rajmohan and Elango 2003). On the other hand, some samples fell below the equiline, indicating

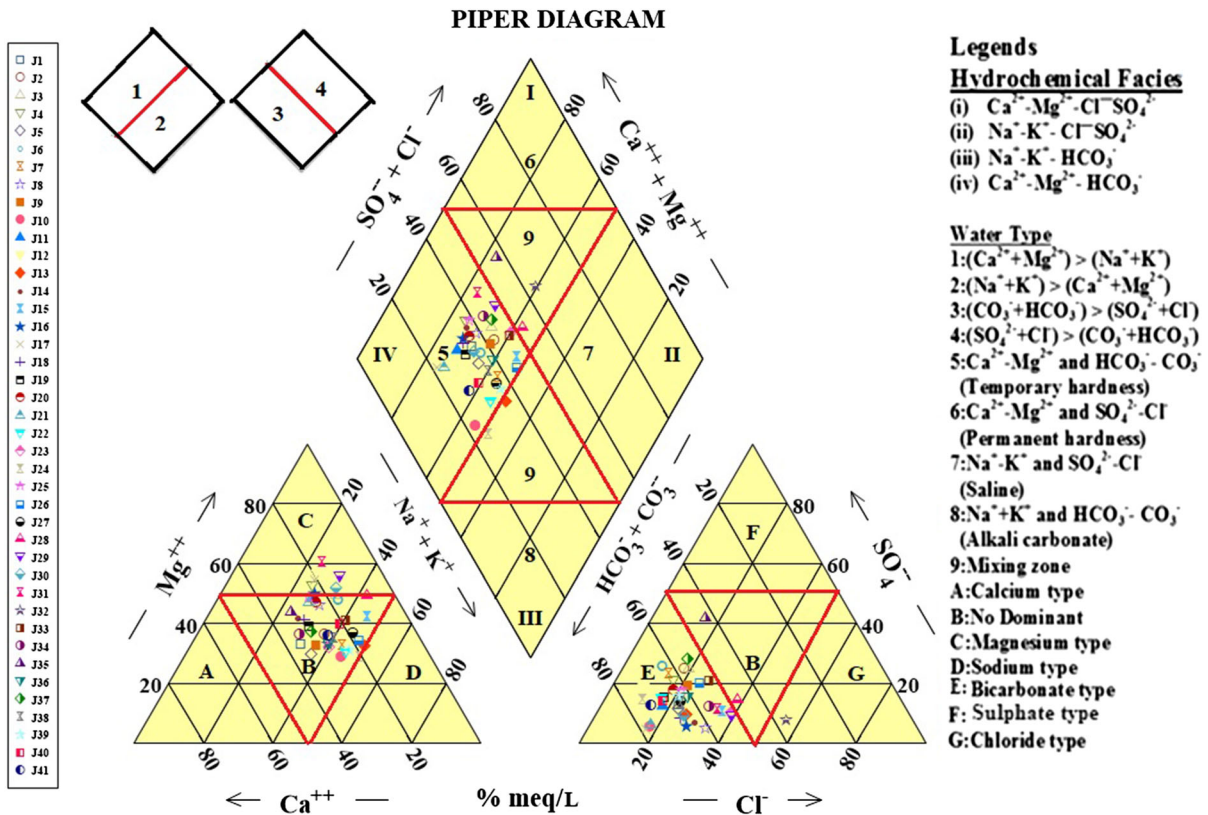
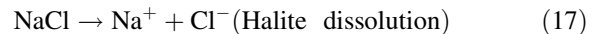
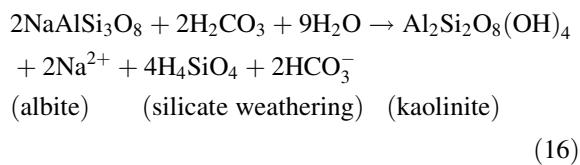


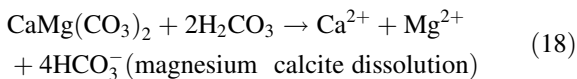
Fig. 11 Piper diagram representing hydrogeochemical facies of groundwater of the study area

the sources of Cl^{-} in the groundwater may be derived from the dissolution of chloride salts (Patel et al. 2016). Some groundwater samples were found on the $y = x$ line, indicating the source of ions is the dissolution of halite as expressed in Eq. 17 (He et al. 2018; Li et al. 2018a). Further, $\text{Na}^{+}/\text{Cl}^{-}$ ratio (Supplementary Table 7) ranged from 0.6 to 4.4 with a mean value of 1.6. Around 78% groundwater samples showed $\text{Na}^{+}/\text{Cl}^{-}$ versus EC (Fig. 9e) ratio more than 1, indicating that silicate weathering is responsible for Na^{+} in the aquifer and 22% groundwater samples showed $\text{Na}^{+}/\text{Cl}^{-}$ versus EC (Fig. 9e) ratio below or close to 1, reflecting that halite dissolution is contributing Na^{+} to the aquifer (Kumar et al. 2015).



The mixing plots of Ca^{2+} normalized Na^{+} versus HCO_3^{-} normalized Na^{+} and Ca^{2+} normalized Na^{+} versus Mg^{2+} normalized Na^{+} reveal silicate weathering is the main factor influencing the aquifer hydrochemistry (Fig. 9f, g). In the scatter plot between SO_4^{2-} and Ca^{2+} (Fig. 9h), most of the samples were below the equiline (1:1), indicating the insignificant amount of gypsum present in the study region (Purushothaman et al. 2014). Few samples were found above the equiline (1:1), indicating the precipitation of calcite, and samples fall along the equiline (1:1), representing the CaSO_4 dissolution (anhydrite) in groundwater (Kumari et al. 2018). The $\text{Ca}^{2+}/\text{Mg}^{2+}$ ratio was also studied to understand the dissolution of dolomite and calcite in the area. Figure 9i depicts that majority of the samples showed the value of $\text{Ca}^{2+}/\text{Mg}^{2+}$ ratio below 1 which indicates dissolution of dolomite is the main process in the alluvial aquifer of

the study area (Mayo and Loucks 1995) and as expressed in Eq. 18.



The high content of magnesium and calcium is largely due to the occurrence of kankar (calcareous encrustations) in the soil matrix of the study region. The scatter plot of $\text{Ca}^{2+} + \text{Mg}^{2+}$ versus total cations (TZ^+) (Fig. 9j) shows that all the groundwater samples were plotted below the equiline (1:1), which indicates that weathering of calcium carbonate (dolomite and calcite) and calc-silicate minerals (plagioclase, amphiboles, pyroxenes) may contribute to Ca^{2+} and Mg^{2+} ions in the alluvial aquifer of the study region (Neogi et al. 2017). Therefore, the reaction of H_2CO_3 with plagioclase feldspar and clinopyroxene acts as an additional source to contribute these ions, namely calcium, magnesium, sodium, bicarbonate and H_4SiO_4 (Eq. 16). In the scatter plot between $\text{Na}^+ + \text{K}^+$ and TZ^+ (Fig. 9k), all the samples were plotted below the equiline ($\text{Na}^+ + \text{K}^+ = 0.5\text{TZ}^+$), which depicts that the weathering of silicate-containing minerals along with some anthropogenic activities is responsible for sodium and potassium ions in the groundwater (Mahaqi et al. 2018).

Saturation index (SI) and Langelier saturation index (LSI)

The Gibbs diagram (Fig. 8) clearly shows that hydro-chemistry of the study area is mainly influenced by interactions of aquifer materials. Under such interactions, rock minerals may contaminate the groundwater (Sridharan and Nathan 2018). The dissolution/precipitation of minerals is the major governing natural process responsible for the major solute in natural water which further depends upon the saturation state of the minerals (Li et al. 2010, 2018a). The chemical equilibrium for a particular mineral is evaluated by the SI using Eq. 19. SI of seven minerals such as calcite, dolomite, aragonite, gypsum, anhydrite, fluorite and halite was estimated by using geochemical modelling software PHREEQC 3.1.2 and is presented in Supplementary Table 7.

$$\text{SI} = \log \text{IAP}/K_{\text{sp}} \quad (19)$$

where IAP is the ion activity product and K_{sp} is the mineral solubility product.

SI value equal to zero indicates saturation, whereas SI value > 0 and SI value < 0 indicate supersaturation (precipitation and saturation from the groundwater) and undersaturation (dissolution of the minerals into groundwater.) with respect to a particular mineral, respectively (Li et al. 2010; Ndoye et al. 2018). The calculated SI values for anhydrite (CaSO_4), fluorite (CaF_2), gypsum ($\text{CaSO}_4 \cdot 2\text{H}_2\text{O}$) and halite (NaCl) ranged from -3.29 to -2.06 , -4.68 to -0.7 , -2.99 to -1.76 and -7.76 to -6.47 , respectively (Supplementary Table 7), which showed negative values ($\text{SI} < 0$) in all the groundwater samples (Fig. 10). It indicates that these minerals are in undersaturation state and weathering of these minerals (rock-water) may continue to release Na^+ , SO_4^{2-} , Cl^- , Ca^{2+} and F^- ions into the groundwater. On the other hand, all the groundwater samples showed positive values ($\text{SI} > 0$) for carbonate rock minerals such as calcite (CaCO_3), dolomite [$\text{CaMg}(\text{CO}_3)_2$] and aragonite (CaCO_3), suggesting that the groundwater of the study area is oversaturated with these minerals. The calculated SI values range from 0.1 to 1.35, 0.35 to 2.79 and -0.4 to 1.2 for calcite, dolomite and aragonite, respectively (Supplementary Table 7). In semi-arid regions, some factors like high temperature, evaporation rate and low rainfall are also responsible for the precipitation of calcite minerals in the groundwater (Rashid et al. 2018). The presence of kankars in the study area is an indicator of calcite precipitation. Thus, the oversaturation of magnesium and calcium bearing minerals leads to the depletion of Ca^{2+} and Mg^{2+} concentration in the aquifer system due to their precipitation. Moreover, gypsum dissolution also releases calcium ions, leading to the oversaturation of the groundwater along with calcite mineral due to the common ion effect (Keesari et al. 2016b; Mushtaq et al. 2018).

LSI (Langelier 1946) is also calculated to understand the dissolution, precipitation and neutral state of the groundwater of the study area. The corrosive nature of water chiefly depends upon the interaction of carbonates with CO_2 . The corresponding concentration of Ca^{2+} , Mg^{2+} and CO_2 in the groundwater deters the conversion of HCO_3^- to CO_3^{2-} . LSI is computed by Eq. 20 and their results are given in Supplementary Table 7.

$$\text{LSI} = \text{pH} - \text{pH}_s \quad (20)$$

where $\text{pH} = -\log[\text{H}^+]$

$$\text{pH}_s = (9.3 + a + b) - (c - d)$$

$$a = \log_{10}(\text{TDS}) - \frac{1}{10}$$

$$b = -13.12 \log_{10}(C + 273) + 34.55$$

$$c = \log_{10}(\text{Ca}^{2+} \text{ as CaCO}_3 \text{ mg/L}) - 0.4$$

$$d = \log_{10}(\text{alkalinity as CaCO}_3 \text{ mg/L})$$

The calculated LSI values ranged from -3.19 to -1.24 , which indicates that all the groundwater samples may readily dissolved the carbonate minerals from the aquifer due to free CO_2 and thus mild to moderate corrosive nature of water (Supplementary Table 6).

Hydrochemical facies of the groundwater

To know the hydrochemical facies and associated processes in the groundwater of the study area, water quality chemical data are plotted on the Piper trilinear diagram (Piper 1944). Table 6 and Fig. 11 show that the majority of the groundwater samples belong to $\text{Ca}^{2+}\text{-Mg}^{2+}\text{-HCO}_3^-$ (87.80%) hydrochemical facies followed by $\text{Ca}^{2+}\text{-Mg}^{2+}\text{-Cl}^- \text{-SO}_4^{2-}$ (7.31%) hydrochemical facies in certain pockets. It indicates that apart from the natural process (weathering of silicates and carbonates, ion exchange process), partially by some anthropogenic activities such as irrigation return flow, septic tank effluents and municipal wastewater, the aquifer salinity is influenced (Selvam et al. 2018). On the other hand, alkaline earth ($\text{Ca}^{2+}\text{-Mg}^{2+}$) significantly exceeds alkalies ($\text{Na}^+\text{-K}^+$) and weak acids ($\text{HCO}_3^- \text{-CO}_3^{2-}$) exceed over the strong acids ($\text{Cl}^- \text{-SO}_4^{2-} \text{-F}^-$) in the study area. About 87.80% samples fall in the 5th field where carbonate hardness (secondary alkalinity) exceeds 50%; it may be due to the silicate weathering in the study area (Herojeet et al. 2017). In cation triangle, 87.80% and 12.19% of groundwater samples fall into the no dominant and Mg^{2+} water type, respectively. Among anions, the majority of the samples (92.62) fall in HCO_3^- water type (Table 6). Thus, the Piper diagram suggests that weathering of silicates and carbonates and cation

exchange process are the main factors governing the hydrochemistry in this study area.

Chemometric analysis

Principal component analysis

To elucidate the potential pollution sources and geochemical signatures influencing the groundwater chemistry, PCA was applied to sixteen variables of the water quality dataset of the study area. Only those principal components having eigenvalue greater than one have been taken into account for the interpretation of PCA (Herojeet et al. 2016; Rajkumar et al. 2018). In total, five principal components were obtained by varimax rotation with Kaiser normalization method (Herojeet et al. 2017; Sahu et al. 2018), altogether accounted for 81.7% of the cumulative variance (Table 7). The variances of principal components PC1, PC2, PC3, PC4 and PC5 are 33.1%, 17%, 14.1%, 10.3% and 7.2%, respectively (Table 7).

The principal component 1(PC1) corresponds to over 33.1% of the total variance with an eigenvalue 5.29, having positive loading with TH, Mg^{2+} , Cl^- and moderate positive loading with EC, TDS and NO_3^- . Strong positive loading of Mg^{2+} and TH indicates that dissolution of dolomite [$\text{CaMg}(\text{CO}_3)_2$] mineral significantly controlling the groundwater chemistry of the study area is also revealed in Fig. 9i. The strong positive loading for Cl^- and moderate positive loading for NO_3^- are mainly attributed to anthropogenic activities chiefly industrial effluents, irrigation return flow and applications of fertilizers as agriculture is the dominant LULC class in the study area (Srinivasamoorthy et al. 2014; Keesari et al. 2016a; Kaur et al. 2019). Moreover, the study area lacks proper sewerage and drainage network; thus, seepages from the septic tanks coupled with domestic and municipal sewage in the aquifer also contribute to these ions (NO_3^- and Cl^-). Overall PC1 describes that both natural (cation exchange, dolomite dissolution) and anthropogenic sources influence the hydrochemistry of the aquifer. PC2 is contributing 17% of the overall variance with an eigenvalue 2.72 in the hydrochemical data of the groundwater. TA and HCO_3^- show strong positive score in PC2 with the loading value of 0.88 and 0.90, respectively. The main source of HCO_3^- is due to silicate weathering and dissolution of carbonate rocks such as calcite [CaCO_3] and dolomite

[CaMg(CO₃)₂] as shown in Eqs. 9, 10, 18 and Fig. 9b (Keesari et al. 2014; Li et al. 2018a). Based on the Piper and box plot diagram, HCO₃⁻ is the dominant anion in the groundwater which influences the TA in the groundwater (Keesari et al. 2014; G et al. 2015; Roy et al. 2018). A moderate positive loading of Na⁺ with TDS and EC indicates that dissolution of silicate and albite minerals are responsible for the Na⁺ in the groundwater of the study area as discussed in Eq. 16 and Fig. 9e. Hence, PC2 is mainly influenced by the natural processes due to weathering and dissolution of calcite, dolomite, silicate and albite minerals. PC3 accounts for 14.1% variance with eigenvalue 2.24 dominated by strong negative loading of pH (- 0.85) and CO₃²⁻ (- 0.75) and moderate positive loading of K⁺ (0.68) and PO₄³⁻ (0.52). The strong correlation between pH and carbonate indicates that CO₃²⁻ is mainly controlled by the pH as alkaline condition favours the formation of the CO₃²⁻ in the groundwater (Raju and Singh 2017). The evapotranspiration process also increases the pH of groundwater (Batabyal and Gupta 2017). The moderate positive loading between K⁺ and PO₄³⁻ indicates that application of potash fertilizers and agrochemicals reflects the anthropogenic origin (Keesari et al. 2016a; Roy et al. 2018). The PC4 contributes 10.3% of the total variance with eigenvalue 1.65 and the strong loading on F⁻ (0.79) and moderate negative weight SO₄²⁻ (- 0.64), suggesting the geogenic and anthropogenic origin. The SI revealed that fluorite and anhydrite mineral is the indicator of F⁻ and SO₄²⁻ content in the groundwater. Moreover, the study area is represented by semi-arid condition; thus, high evaporation rate and longer residence time of groundwater (water-rock interaction under alkaline condition) are the significant factors for the fluoride in the region (Purushothaman et al. 2014; Adimalla and Li 2018; Khanoranga 2019). The negative loading of Ca²⁺ with respect to F⁻ is due to the process of oversaturation of calcite mineral, which leads to the precipitation of CaCO₃ and promotes the dissolution of CaF₂⁻ mineral. After oversaturation, the process of common ion effect suppresses the CaF₂ dissolution and this condition gave negative loading of Ca²⁺ with F⁻ (Batabyal and Gupta 2017). Insignificant loading of F⁻ with other variables neglected the anthropogenic influence in groundwater chemistry. However, the inverse relation of SO₄²⁻ and the absence of correlation with other parameters indicate the different sources of origin

related to human activities (Brindha et al. 2017). A strong positive loading observed in Ca²⁺ in PC5 represents 7.2% of the entire variance with eigenvalue 1.1. It is mainly influenced by the natural processes such as the dissolution of calcite and limestone (kankars) along with the cation exchange process, significantly contributing to the calcium concentration in the study area.

Cluster analysis

CA is performed to categorize the analyse dataset of groundwater samples. Four clusters were identified by dendrogram and their significance was further studied by the Sneath's test techniques (D_{link}/D_{max})*100 < 90 (Supplementary Fig. 4). To elucidate the heterogeneity among the clustering pattern, the mean value of each physiochemical parameters is computed for individual cluster group (Table 8). The indicator parameters influencing each clustering pattern are marked bold and italics with bold.

Cluster 1 (C1) represents the largest number of sampling group accounting 56.09% of the total samples. SO₄²⁻ is the only special tracer influencing C1 which indicates that this ion might have different sources rather than geogenic factor. Saturation index revealed that dissolution of anhydrite mineral releases SO₄²⁻ ion which is in undersaturation. However, the absence of any significant relation with other parameter depicts the contribution from human induce sources such as the by-products of fertilizer, breakdown of organic materials from weathered soil releasing sulphate into groundwater as the study area being intensively cultivated region. C2 forms the highest levels of pH and CO₃²⁻ and higher value of TA comprises 21.95% of the samples. It signifies that the presence of CO₃⁻ ion is controlled by pH (alkaline conditions) which further influenced TA in groundwater (Roy et al. 2018). Therefore, the samples locations belong to C2 which indicates alkaline nature of water. The third cluster (C3) is marked by the special tracers of Mg²⁺, HCO₃⁻ and TA and higher levels of Ca²⁺ and TH which constitutes 12.21% of the entire samples. The significance level of Ca²⁺, Mg²⁺ and HCO₃⁻ depicts temporary hardness. However, the presence of dominant HCO₃⁻ ion is the main reason for TA and fits well with PC2. Piper diagram revealed that temporary hardness (Ca²⁺-Mg²⁺-HCO₃⁻ water type) in groundwater is found in C3. The last cluster (C4) is formed by the single sampling location (32) with

multiple parameter tracers, namely EC, TDS, TH, Ca^{2+} , Na^+ , K^+ , NO_3^- , F^- , Cl^- and PO_4^{3-} , respectively. The excess content of these parameters makes the water highly mineralized, resulting in high EC and TDS. The main source of Ca^{2+} , Na^+ , K^+ and F^- is the geogenic source, whereas NO_3^- , Cl^- and PO_4^{3-} belong to anthropogenic inputs as discussed above. The groundwater of this sampling location falls under salinity class as per the Revelle index. Therefore, C4 is influenced by salinity problem. Chemometric statistical techniques (PCA and CA) confirmed that the groundwater samples are largely controlled by parameters Ca^{2+} , Mg^{2+} , Na^+ , K^+ , HCO_3^- , CO_3^- and F^- originated from geogenic factors and NO_3^- , SO_4^{2-} , Cl^- and PO_4^{3-} of anthropogenic origin with minor influenced on the aquifer.

Conclusion

The groundwater is the main source for drinking and other purposes in the study area. Extensive agricultural activities and overextraction of groundwater draws the main attention for suitability appraisal using integrated application of GIS and chemometric statistical techniques and human health risk assessment through direct ingestion of groundwater. The analytical result of the physicochemical parameters revealed that the majority of the groundwater samples are within the permissible limits of BIS (2012) and WHO (2011), except few samples of pH, NO_3^- and F^- , respectively. The calculated DWQI exhibited that 49% of the groundwater samples fall under poor to unfit for drinking class. The corroboration of DWQI and RI results depicted that poor water quality zones are the south-western and central parts of the study area that may be influenced by groundwater movement, leading to salinization besides local pollution sources. The groundwater chemistry is mainly governed by rock–water interaction, indicating Ca^{2+} – Mg^{2+} – HCO_3^- is the dominant hydrochemical facies with Mg^{2+} – HCO_3^- water type in the study area. The non-carcinogenic human health risk assessment shows that ~ 68% groundwater samples have shown $\text{HI} > 1$ and their mean value of $\text{HI}_{\text{ingestion}}$ indicates that children are more vulnerable to NO_3^- and F^- contaminants than adults through direct ingestion of groundwater. Chemometric statistical analysis and bivariate plots between different ions revealed that in addition to the natural processes such as weathering of silicate and carbonate minerals, halite dissolution and cation

exchange process, some anthropogenic factors also influence the groundwater chemistry of the region. It is recommended that the study of groundwater quality must be assessed together with RI and groundwater movement. Further, the poor water quality zones of south-western and central part must be properly treated before subjected to drinking purpose. Due to the agriculture-based economy and lack of proper education and awareness related to water quality, the potential public health risks are often ignored in the study area as well as other parts of the country. This integrative study is a noble approach to understand groundwater quality, salinity related to flow direction and pollution source extraction to demarcate the aquifer region for immediate restoration and management formulation and policy as well. The future dimensions of the study shall be focused on human health risks associated with heavy metals contamination in groundwater and soil. Regular monitoring is vital for sustainable groundwater management and long-term protection of water quality from further deterioration.

Acknowledgements The University Grant Commission (UGC), Government of India, is duly acknowledged for providing Rajiv Gandhi National Fellowship (UGC-RGNF) for the doctoral degree. The author would like to express special thanks to Mr. Kuldeep Bist, Centre of Advance Study in Geology, Panjab University, Chandigarh, for his help during the chemical analysis.

Compliance with ethical standards

Conflict of interest The authors declare that they have no conflict of interest.

References

- Adimalla, N. (2018). Groundwater quality for drinking and irrigation purposes and potential health risks assessment: A case study from semi-arid region of South India. *Exposure and Health*. <https://doi.org/10.1007/s12403-018-0288-8>.
- Adimalla, N., & Li, P. (2018). Occurrence, health risks, and geochemical mechanisms of fluoride and nitrate in groundwater of the rock-dominant semi-arid region, Telangana State, India. *Human and Ecological Risk Assessment*. <https://doi.org/10.1080/10807039.2018.1480353>.
- Adimalla, N., Li, P., & Venkatayogi, S. (2018). Hydrogeochemical evaluation of groundwater quality for drinking and irrigation purposes and integrated interpretation with water quality index studies. *Environmental Processes*, 5, 363–383. <https://doi.org/10.1007/s40710-018-0297-4>.

- Ahada, C. P. S., & Suthar, S. (2018a). Assessing groundwater hydrochemistry of Malwa Punjab India. *Arabian Journal of Geosciences*. <https://doi.org/10.1007/s12517-017-3355-8>.
- Ahada, C. P. S., & Suthar, S. (2018b). Groundwater nitrate contamination and associated human health risk assessment in southern districts of Punjab, India. *Environmental Science and Pollution Research*, 25, 25336–25347. <https://doi.org/10.1007/s11356-018-2581-2>.
- Ahmed, M. F., Bin, Mokhtar M., Alam, L., et al. (2019). Non-carcinogenic health risk assessment of aluminium ingestion via drinking water in Malaysia. *Exposure and Health*. <https://doi.org/10.1007/s12403-019-00297-w>.
- American Public Health Association. APHA. (2005). *Standard methods for the examination of water and wastewater* (21st ed.). Washington, DC: American Public Health Association.
- Aulakh, M. S., Khurana, M. P. S., & Singh, D. (2009). Water pollution related to agricultural, industrial, and urban activities, and its effects on the food chain: case studies from punjab. *Journal of New Seeds*, 10, 112–137. <https://doi.org/10.1080/15228860902929620>.
- Aydi, A. (2018). Evaluation of groundwater vulnerability to pollution using a GIS-based multi-criteria decision analysis. *Groundwater for Sustainable Development*, 7, 204–211. <https://doi.org/10.1016/j.gsd.2018.06.003>.
- Batabyal, A. K., & Gupta, S. (2017). Fluoride-contaminated groundwater of Birbhum district, West Bengal, India: interpretation of drinking and irrigation suitability and major geochemical processes using principal component analysis. *Environmental Monitoring and Assessment*, 189, 369. <https://doi.org/10.1007/s10661-017-6041-0>.
- Brindha, K., Pavelic, P., Sotoukee, T., et al. (2017). Geochemical characteristics and groundwater quality in the vientiane plain, Laos. *Exposure and Health*, 9, 89–104. <https://doi.org/10.1007/s12403-016-0224-8>.
- Bureau of Indian Standards (BIS) (2012). Specification for drinking water. IS: 10500. Bureau of Indian Standards, New Delhi.
- Causapé, J., Quílez, D., & Aragü, R. (2006). Groundwater quality in CR-V irrigation district (Bardenas I, Spain): Alternative scenarios to reduce off-site salt and nitrate contamination. *Agricultural Water Management*. <https://doi.org/10.1016/j.agwat.2006.03.004>.
- Central Ground Water Board (CGWB) (2012). Aquifer systems of India. 111.
- CGWB (2014). Dynamic Groundwater Resources of India (As on March 31st 2011). Cent Gr Water Board Minist Water Resour River Dev Ganga Rejuvenation Gov India 299.
- CGWB (2016). Ground Water Year Book, Punjab and Chandigarh. 186.
- CGWB (2018). Aquifer mapping and management plan Jalandhar district, Punjab, CGWB, Ministry of Water Resources, Government of India.
- Chen, J., Wu, H., Qian, H., & Gao, Y. (2017). Assessing nitrate and fluoride contaminants in drinking water and their health risk of rural residents living in a semiarid region of northwest China. *Exposure and Health*, 9, 183–195. <https://doi.org/10.1007/s12403-016-0231-9>.
- Das, B., & Kaur, P. (2001). Major ion chemistry of Renuka Lake and weathering processes, Sirmour District, Himachal Pradesh, India. *Environmental Geology*, 40, 908–917. <https://doi.org/10.1007/s002540100268>.
- Davis, S. N., & DeWiest, R. J. M. (1967). *Hydrology* (2nd ed., p. 463). New York, London.
- Dhillon, M. S., Kaur, S., & Aggarwal, R. (2019). Delineation of critical regions for mitigation of carbon emissions due to groundwater pumping in central Punjab. *Groundwater for Sustainable Development*, 8, 302–308. <https://doi.org/10.1016/j.gsd.2018.11.010>.
- Emenike, C. P., Tenebe, I. T., & Jarvis, P. (2018). Fluoride contamination in groundwater sources in Southwestern Nigeria: Assessment using multivariate statistical approach and human health risk. *Ecotoxicology and Environmental Safety*, 156, 391–402.
- Freeze, R. A., & Cherry, J. A. (1979). *Groundwater*. Englewood Cliffs: Prentice-Hall.
- Gaofeng, Z., Yonghong, S., Chunlin, H., et al. (2010). Hydrogeochemical processes in the groundwater environment of Heihe River Basin, northwest China. *Environmental Earth Sciences*, 60, 139–153. <https://doi.org/10.1007/s12665-009-0175-5>.
- Gibbs, R. J. (1970). Mechanisms controlling world water chemistry. *Science*, 170, 1088–1090. <https://doi.org/10.1126/science.170.3962.1088>.
- Government of Punjab (2016). STATISTICAL ABSTRACT OF Punjab, 2016.
- He, S., & Wu, J. (2018). *Hydrogeochemical characteristics, groundwater quality, and health risks from hexavalent chromium and nitrate in groundwater of huanhe formation in Wuqi County*. Northwest China: Exposure and Health. <https://doi.org/10.1007/s12403-018-0289-7>.
- He, X., Wu, J., & He, S. (2018). Hydrochemical characteristics and quality evaluation of groundwater in terms of health risks in Luohe aquifer in Wuqi County of the Chinese Loess Plateau, northwest China. *Human and Ecological Risk Assessment: An International Journal*. <https://doi.org/10.1080/10807039.2018.1531693>.
- Herojeet, R., Rishi, M. S., & Kishore, N. (2015). Integrated approach of heavy metal pollution indices and complexity quantification using chemometric models in the Sirsa Basin, Nalagarh valley, Himachal Pradesh, India. *Chinese J Geochemistry*, 34, 620–633. <https://doi.org/10.1007/s11631-015-0075-1>.
- Herojeet, R., Rishi, M. S., Lata, R., & Dolma, K. (2017). Quality characterization and pollution source identification of surface water using multivariate statistical techniques, Nalagarh Valley, Himachal Pradesh, India. *Applied Water Science*, 7, 2137–2156. <https://doi.org/10.1007/s13201-017-0600-y>.
- Herojeet, R., Rishi, M. S., Lata, R., & Sharma, R. (2016). Application of environmetrics statistical models and water quality index for groundwater quality characterization of alluvial aquifer of Nalagarh Valley, Himachal Pradesh, India. *Sustainable Water Resources Management*, 2, 39–53. <https://doi.org/10.1007/s40899-015-0039-y>.
- Horton, R. K. (1965). An index number system for rating water quality. *Journal of Water Pollution Control Federation*, 37(3), 300–306.
- Hounslow, A. (2018). *Water quality data: analysis and interpretation*. Boca Raton: CRC Press.

- Jain, C. K., & Vaid, U. (2018). Assessment of groundwater quality for drinking and irrigation purposes using hydrochemical studies in Nalbari district of Assam India. *Environmental Earth Sciences*. <https://doi.org/10.1007/s12665-018-7422-6>.
- Karant, K. R. (1987). *Ground water assessment, development, and management*. New York: Tata McGraw-Hill Pub co.
- Kaur, L., & Rishi, M. S. (2018). Integrated geospatial, geostatistical, and remote-sensing approach to estimate groundwater level in North-western India. *Environmental Earth Sciences*, 77, 786. <https://doi.org/10.1007/s12665-018-7971-8>.
- Kaur, L., Rishi, M. S., Sharma, S., et al. (2019). Hydrogeochemical characterization of groundwater in alluvial plains of River Yamuna in Northern India: an insight of controlling processes. *Journal of King Saud University-Science*. <https://doi.org/10.1016/J.KJSUS.2019.01.005>.
- Keesari, T., Kulkarni, U. P., Deodhar, A., et al. (2014). Geochemical characterization of groundwater from an arid region in India. *Environmental Earth Sciences*, 71, 4869–4888. <https://doi.org/10.1007/s12665-013-2878-x>.
- Keesari, T., Ramakumar, K. L., Chidambaram, S., et al. (2016a). Understanding the hydrochemical behavior of groundwater and its suitability for drinking and agricultural purposes in Pondicherry area, South India—A step towards sustainable development. *Groundwater for Sustainable Development*, 2–3, 143–153. <https://doi.org/10.1016/j.gsd.2016.08.001>.
- Keesari, T., Sinha, U. K., Deodhar, A., et al. (2016b). High fluoride in groundwater of an industrialized area of Eastern India (Odisha): inferences from geochemical and isotopic investigation. *Environmental Earth Sciences*. <https://doi.org/10.1007/s12665-016-5874-0>.
- Keesari, T., Sinha, U. K., Kamaraj, P., & Sharma, D. A. (2019). Groundwater quality in a semi-arid region of India: Suitability for drinking, agriculture and fluoride exposure risk. *Journal of Earth System Science*, 128(2), 24.
- Khanoranga, Khalid S. (2019). An assessment of groundwater quality for irrigation and drinking purposes around brick kilns in three districts of Balochistan province, Pakistan, through water quality index and multivariate statistical approaches. *Journal of Geochemical Exploration*, 197, 14–26. <https://doi.org/10.1016/j.gexplo.2018.11.007>.
- Kumar, P., Kumar, S., & Joshi, L. (2015). Problem of residue management due to rice wheat crop rotation in Punjab. In *Socioeconomic and Environmental Implications of Agricultural Residue Burning* (pp. 1–12). Springer, New Delhi.
- Kumari, R., Datta, P. S., Rao, M. S., et al. (2018). Anthropogenic perturbations induced groundwater vulnerability to pollution in the industrial Faridabad District, Haryana India. *Environmental Earth Sciences*. <https://doi.org/10.1007/s12665-018-7368-8>.
- Langelier, W.F. (1946). Chemical Equilibria in Water Treatment. In: Am. Water Work. Assoc. <http://www.jstor.org/stable/23349196>. Retrieved 5 Jan 2019.
- Li, P., He, S., Yang, N., & Xiang, G. (2018a). Groundwater quality assessment for domestic and agricultural purposes in Yan'an City, northwest China: Implications to sustainable groundwater quality management on the Loess Plateau. *Environmental Earth Sciences*, 77, 775. <https://doi.org/10.1007/s12665-018-7968-3>.
- Li, P., Qian, H., Wu, J., & Ding, J. (2010). Geochemical modeling of groundwater in southern plain area of Pengyang County, Ningxia, China. *Water Science and Engineering*, 3, 282–291. <https://doi.org/10.3882/j.issn.1674-2370.2010.03.004>.
- Li, P., Wu, J., Qian, H., et al. (2016). Hydrogeochemical characterization of groundwater in and around a wastewater irrigated forest in the southeastern edge of the Tengger Desert, Northwest China. *Exposure and Health*, 8, 331–348. <https://doi.org/10.1007/s12403-016-0193-y>.
- Li, P., Wu, J., Tian, R., et al. (2018b). Geochemistry, hydraulic connectivity and quality appraisal of multilayered groundwater in the hongdunzi coal mine, northwest China. *Mine Water and the Environment*, 37, 222–237. <https://doi.org/10.1007/s10230-017-0507-8>.
- Liao, F., Wang, G., Shi, Z., et al. (2018). Distributions, sources, and species of heavy metals/trace elements in shallow groundwater around the poyang lake, east China. *Exposure and Health*, 10, 211–227. <https://doi.org/10.1007/s12403-017-0256-8>.
- Mahaqi, A., Moheghi, M. M., Mehiqi, M., & Moheghi, M. A. (2018). Hydrogeochemical characteristics and groundwater quality assessment for drinking and irrigation purposes in the Mazar-i-Sharif city North Afghanistan. *Applied Water Science*, 8, 133. <https://doi.org/10.1007/s13201-018-0768-9>.
- Margat, J., & Van der Gun, J. (2013). *Groundwater around the world: A geographic synopsis*. Boca Raton: CRC Press.
- Mayo, A. L., & Loucks, M. D. (1995). Solute and isotopic geochemistry and ground water flow in the central Wasatch Range, Utah. *Journal of Hydrology*, 172, 31–59. [https://doi.org/10.1016/0022-1694\(95\)02748-E](https://doi.org/10.1016/0022-1694(95)02748-E).
- Mohamed, I., Othman, F., Ibrahim, A. I. N., et al. (2015). Assessment of water quality parameters using multivariate analysis for Klang River basin, Malaysia. *Environmental Monitoring and Assessment*, 187, 1–12. <https://doi.org/10.1007/s10661-014-4182-y>.
- Mukate, S., Panaskar, D., Wagh, V., et al. (2018). Impact of anthropogenic inputs on water quality in Chincholi industrial area of Solapur, Maharashtra, India. *Groundwater for Sustainable Development*, 7, 359–371. <https://doi.org/10.1016/j.gsd.2017.11.001>.
- Mushtaq, N., Younas, A., Mashiattullah, A., et al. (2018). Hydrogeochemical and isotopic evaluation of groundwater with elevated arsenic in alkaline aquifers in Eastern Punjab, Pakistan. *Chemosphere*, 200, 576–586. <https://doi.org/10.1016/j.chemosphere.2018.02.154>.
- Nagaraju, A., Sunil Kumar, K., Thejaswi, A., & Sharifi, Z. (2014). Statistical analysis of the hydrogeochemical evolution of groundwater in the Rangampeta area, Chittoor District, Andhra Pradesh, South India. *American Journal of Water Resources*, 2, 63–70. <https://doi.org/10.12691/ajwr-2-3-2>.
- Ndoye, S., Fontaine, C., Gaye, C., & Razack, M. (2018). Groundwater quality and suitability for different uses in the Saloum Area of Senegal. *Water*, 10, 1837. <https://doi.org/10.3390/w10121837>.
- Neogi, B., Singh, A. K., Pathak, D. D., & Chaturvedi, A. (2017). Hydrogeochemistry of coal mine water of North Karanpura coalfields, India: implication for solute acquisition processes, dissolved fluxes and water quality assessment.

- Environmental Earth Sciences*, 76, 1–17. <https://doi.org/10.1007/s12665-017-6813-4>.
- Otto, M. (1998). Multivariate methods. In R. Kellner, J. M. Mermet, M. Otto, & H. M. Widmer (Eds.), *Analytical chemistry*. Weinheim: Wiley-VCH.
- Pant, D., Keesari, T., Sharma, D., et al. (2017a). Study on uranium contamination in groundwater of Faridkot and Muktsar districts of Punjab using stable isotopes of water. *Journal of Radioanalytical and Nuclear Chemistry*, 313, 635–639. <https://doi.org/10.1007/s10967-017-5284-0>.
- Pant, D., Keesari, T., Rishi, M., et al. (2019). Spatiotemporal distribution of dissolved radon in uranium impacted aquifers of southwest Punjab. *Journal of Radioanalytical and Nuclear Chemistry*. <https://doi.org/10.1007/s10967-019-06656-w>.
- Pant, D., Tirumalesh, K., Kumar, A., et al. (2017b). Environmental isotopic study on uranium contamination in groundwater of Faridkot and Muktsar Districts of Punjab. In *Proceedings of the thirteenth DAE-BRNS nuclear and radiochemistry symposium*.
- Patel, P., Raju, N. J., Reddy, B. C. S. R., et al. (2016). Geochemical processes and multivariate statistical analysis for the assessment of groundwater quality in the Swarnamukhi River basin, Andhra Pradesh India. *Environmental Earth Sciences*, 75, 611. <https://doi.org/10.1007/s12665-015-5108-x>.
- Piper, A. M. (1944). A graphic procedure in the geochemical interpretation of water-analyses Transactions. *American Geophysical Union*, 25, 914. <https://doi.org/10.1029/TR025i006p00914>.
- Purushothaman, P., Someshwar Rao, M., Kumar, B., et al. (2012). Drinking and irrigation water quality in Jalandhar and Kapurthala Districts, Punjab, India: using hydrochemistry. *International Journal of Earth Sciences and Engineering*, 5, 1599–1608. <https://doi.org/10.1509/jppm.27.2.117>.
- Purushothaman, P., Someshwar Rao, M., Rawat, Y. S., et al. (2014). Evaluation of hydrogeochemistry and water quality in Bist-Doab region, Punjab, India. *Environmental Earth Sciences*, 72, 693–706. <https://doi.org/10.1007/s12665-013-2992-9>.
- Rahman, M. M., Islam, M. A., Bodrud-Doza, M., et al. (2018). Spatio-temporal assessment of groundwater quality and human health risk: A case study in Gopalganj, Bangladesh. *Exposure and Health*, 10, 167–188. <https://doi.org/10.1007/s12403-017-0253-y>.
- Rajkumar, H., Naik, P. K., & Rishi, M. S. (2018). Evaluation of heavy metal contamination in soil using geochemical indexing approaches and chemometric techniques. *International Journal of Environmental Science and Technology*. <https://doi.org/10.1007/s13762-018-2081-4>.
- Rajmohan, N., & Elango, L. (2003). Identification and evolution of hydrogeochemical processes in the groundwater environment in an area of the Palar and Cheyyar River Basins, Southern India. *Environmental Geology*. <https://doi.org/10.1007/s00254-004-1012-5>.
- Raju, A., & Singh, A. (2017). Assessment of groundwater quality and mapping human health risk in central Ganga Alluvial Plain, Northern India. *Environmental Processes*, 4, 375–397. <https://doi.org/10.1007/s40710-017-0232-0>.
- Rao, M. S., Krishan, G., Kumar, C. P., et al. (2017). Observing changes in groundwater resource using hydro-chemical and isotopic parameters: a case study from Bist Doab, Punjab. *Environmental Earth Sciences*, 76, 1–16. <https://doi.org/10.1007/s12665-017-6492-1>.
- Rao, S., Mahesh, J., Surinaidu, L., & Dhakate, R. (2015). Hydrochemical assessment of groundwater in alluvial aquifer region, Jalandhar District, Punjab, India. *Environmental Earth Sciences*, 73(12), 8145–8153.
- Rashid, A., Guan, D. X., Farooqi, A., et al. (2018). Fluoride prevalence in groundwater around a fluorite mining area in the flood plain of the River Swat, Pakistan. *Science of the Total Environment*, 635, 203–215. <https://doi.org/10.1016/j.scitotenv.2018.04.064>.
- Revelle, R. (1941). Criteria for recognition of the sea water in ground-waters. *EOS, Transactions of the American Geophysical Union*, 22, 593–597. <https://doi.org/10.1029/TR022i003p00593>.
- Roy, A., Keesari, T., Mohokar, H., et al. (2018). Assessment of groundwater quality in hard rock aquifer of central Telangana state for drinking and agriculture purposes. *Applied Water Science*, 8, 124. <https://doi.org/10.1007/s13201-018-0761-3>.
- Sahu, P., Kisku, G. C., Singh, P. K., et al. (2018). Multivariate statistical interpretation on seasonal variations of fluoride-contaminated groundwater quality of Lalganj Tehsil, Raebareli District (UP) India. *Environmental Earth Sciences*, 77, 484. <https://doi.org/10.1007/s12665-018-7658-1>.
- Sawyer, C. N., & McCarty, D. L. (1967). *Chemistry of sanitary engineers* (2nd ed., p. 518). New York: McGraw-Hill.
- Selvam, S., Singaraja, C., Venkatramanan, S., & Chung, S. Y. (2018). Geochemical appraisal of groundwater quality in Ottapidaram Taluk Thoothukudi District, Tamil Nadu using graphical and numerical method. *Journal of the Geological Society of India*, 92, 313–320. <https://doi.org/10.1007/s12594-018-1013-8>.
- Shakerkhatibi, M., Mosaferi, M., Pourakbar, M., et al. (2019). Comprehensive investigation of groundwater quality in the north-west of Iran: physicochemical and heavy metal analysis. *Groundwater for Sustainable Development*, 8, 156–168. <https://doi.org/10.1016/J.GSD.2018.10.006>.
- Sharma, S., Rishi, M.S., Kaur, L., & Singh, G. (2017). Resource development and management of groundwater focusing sustainability issues in Urban City. 12:887–900.
- Singh, C. K., Kumar, A., Shashtri, S., et al. (2017). Multivariate statistical analysis and geochemical modeling for geochemical assessment of groundwater of Delhi, India. *Journal of Geochemical Exploration*, 175, 59–71. <https://doi.org/10.1016/j.gexplo.2017.01.001>.
- Singh, K. P., Malik, A., Mohan, D., & Sinha, S. (2004). Multivariate statistical techniques for the evaluation of spatial and temporal variations in water quality of Gomti River (India)—A case study. *Water Research*, 38, 3980–3992. <https://doi.org/10.1016/j.watres.2004.06.011>.
- Singh, A., Sharma, C. S., Jeyaseelan, A. T., & Chowdary, V. M. (2015). Spatio-temporal analysis of groundwater resources in Jalandhar district of Punjab state, India. *Sustainable Water Resources Management*, 1, 293–304. <https://doi.org/10.1007/s40899-015-0022-7>.

- Singh, P.K., Verma, P., & Tiwari, A.K. (2018). Hydrogeochemical investigation and qualitative assessment of groundwater resources in Bokaro district, Jharkhand, India.
- Singh, G., Rishi, M. S., & Arora, N. K. (2019a). Integrated GIS-based modelling approach for irrigation water quality suitability zonation in parts of Satluj River Basin, Bist Doab region, North India. *SN Applied Sciences*, *1*(11), 1438.
- Singh, G., Rishi, M. S., Herojeet, R., Kaur, L., & Sharma, K. (2019b). Multivariate analysis and geochemical signatures of groundwater in the agricultural dominated taluks of Jalandhar district, Punjab, India. *Journal of Geochemical Exploration*, 106395.
- Song, Y., Li, H., Li, J., et al. (2018). Multivariate linear regression model for source apportionment and health risk assessment of heavy metals from different environmental media. *Ecotoxicology and Environmental Safety*, *165*, 555–563. <https://doi.org/10.1016/j.ecoenv.2018.09.049>.
- Sridharan, M., & Nathan, D. S. (2018). Chemometric tool to study the mechanism of arsenic contamination in groundwater of Puducherry region, South East coast of India. *Chemosphere*, *208*, 303–315. <https://doi.org/10.1016/j.chemosphere.2018.05.083>.
- Srinivasamoorthy, K., Gopinath, M., Chidambaram, S., et al. (2014). Hydrochemical characterization and quality appraisal of groundwater from Pungar sub basin, Tamilnadu, India. *Journal of King Saud University-Science*, *26*, 37–52. <https://doi.org/10.1016/J.JKSUS.2013.08.001>.
- Tiwari, T. N., & Mishra, M. A. (1985). A preliminary assignment of water quality index of major Indian rivers. *Indian Journal of Environmental Protection*, *5*(4), 276–279.
- U.S. EPA (U.S. Environmental Protection Agency) (2009). Risk Assessment Guidance for Superfund, Human Health Evaluation Manual. I:1–68. doi: [EPA/540/1-89/002].
- World Bank (2012). India groundwater: A valuable but diminishing resource.
- Wu, J., & Sun, Z. (2016). Evaluation of shallow groundwater contamination and associated human health risk in an alluvial plain impacted by agricultural and industrial activities, mid-west China. *Exposure and Health*, *8*, 311–329. <https://doi.org/10.1007/s12403-015-0170-x>.
- Yadav, K. K., Gupta, N., Kumar, V., et al. (2018). GIS-based evaluation of groundwater geochemistry and statistical determination of the fate of contaminants in shallow aquifers from different functional areas of Agra city, India: levels and spatial distributions. *RSC Advances*, *8*, 15876–15889. <https://doi.org/10.1039/C8RA00577J>.

Publisher's Note Springer Nature remains neutral with regard to jurisdictional claims in published maps and institutional affiliations.